

Paleoceanography and Paleoclimatology

RESEARCH ARTICLE

10.1029/2022PA004510

Key Points:

- Grain size End-Member Mixing Analysis (EMMA) permits recognition of major storm and heavy rainfall events in an ~500 years lake core record
- CONISS zonation of EMMA and ITRAX data from core delineated phases of the Little Ice Age (LIA) and transition to modern warm era
- Storm records and major rain events characterized LIAa, then nearly ceased before increasing dramatically during the modern warm era

Supporting Information:

Supporting Information may be found in the online version of this article.

Correspondence to:

R. T. Patterson,
tim.patterson@carleton.ca

Citation:

Patterson, R. T., Nasser, N. A., Reinhardt, E. G., Patterson, C. W., Gregory, B. R. B., Mazzella, V., et al. (2022). End-member mixing analysis as a tool for the detection of major storms in lake sediment records. *Paleoceanography and Paleoclimatology*, 37, e2022PA004510. <https://doi.org/10.1029/2022PA004510>


Received 19 JUL 2022
Accepted 17 OCT 2022

Author Contributions:

Conceptualization: R. Timothy Patterson
Data curation: R. Timothy Patterson, Nawaf A. Nasser
Formal analysis: R. Timothy Patterson, Nawaf A. Nasser, Eduard G. Reinhardt, Calder W. Patterson, Braden R. B. Gregory, Veronica Mazzella
Funding acquisition: R. Timothy Patterson
Investigation: R. Timothy Patterson, Calder W. Patterson, Braden R. B. Gregory, Veronica Mazzella, Helen M. Roe, Jennifer M. Galloway
Methodology: R. Timothy Patterson, Nawaf A. Nasser, Eduard G. Reinhardt, Calder W. Patterson, Braden R. B. Gregory, Helen M. Roe, Jennifer M. Galloway

© 2022. American Geophysical Union.
All Rights Reserved.

End-Member Mixing Analysis as a Tool for the Detection of Major Storms in Lake Sediment Records

R. Timothy Patterson¹ , Nawaf A. Nasser¹, Eduard G. Reinhardt², Calder W. Patterson³, Braden R. B. Gregory¹, Veronica Mazzella¹, Helen M. Roe⁴, and Jennifer M. Galloway⁵

¹Ottawa-Carleton Geoscience Centre and Department of Earth Sciences, Carleton University, Ottawa, ON, Canada, ²School of Geography and Earth Sciences, McMaster University, Hamilton, ON, Canada, ³Department of Geography and Environmental Studies, Carleton University, Ottawa, ON, Canada, ⁴School of Natural and Built Environment, Queen's University Belfast, Belfast, UK, ⁵Geological Survey of Canada (GSC)/Commission géologique du Canada, Natural Resources Canada (NRCan)/Ressources naturelles Canada (RNCan), Calgary, AB, Canada

Abstract Major Tropical Cyclone (TC) events cause extensive damage in coastal regions of the western North Atlantic Basin. The short instrumental record leaves significant gaps in understanding long-term trends in TC recurrence and intensity, creating uncertainty about future storm trends. Analysis of an ~520-year core record from Harvey Lake, located >80 km from the Atlantic coast in southwestern New Brunswick, Canada was carried out using: (a) end-member mixing analysis (EMMA) of lake sediment grain size data to identify storm-linked sedimentological processes; and (2) ITRAX X-ray fluorescence (XRF) derived element/ratios (Fe, Ti, Ca/Sr, Zr/Rb, K/Rb, and Br + Cl/Al) associated with precipitation, weathering, catchment runoff, and air masses. Three derived end members were correlated to heavy rainfall events (EM01), spring freshet (EM02), and TCs (EM03). CONISS analysis of the EMMA and XRF core data resulted in recognition of four unique climatic zones distinguished by distinct distributions of TC and rainfall/weathering/runoff/and air masses. Numerous, major (EM01) rainfall events and (EM03) TC events characterized the basal core record during the early Little Ice Age (LIAa; Zone 1) phase, terminating at ~1645. A near cessation of heavy rainfall and TC events differentiated the subsequent colder LIAb (~1645–1825; Zone 2) and subsequent Little Ice Age Transition (~1825–1895; Zone 3). A resurgence of major rainfall and TC events occurred during recovery from the LIA starting in ~1895 (Zone 4). EMMA provides a robust tool for recognition of TC and major rainfall events, and greatly expands the potential for paleo-storm activity research well inland from coastal regions.

1. Introduction

Tropical Cyclone (TC) events are an annual seasonal component of the climate system in the western North Atlantic Basin (WNAB), where strikes in coastal regions are inevitable. An understanding of the dynamics of previous TC events (including hurricanes, tropical and extratropical storms) in the WNAB is hampered by the short instrumental record which leaves significant gaps in understanding long-term trends in TC recurrence and intensity. Obtaining such data is critical, as it provides insight into the possible intensity of future events. Such research is critical as the high winds, precipitation, and storm surges associated with TCs in the Caribbean, Gulf of Mexico, and along the eastern seaboard of North America can destroy infrastructure and alter landscapes and ecosystems (Oliva et al., 2017; D. J. Wallace et al., 2014). Despite the significant TC threat, coastal development in this region continues to intensify. For example, the coastal population of US states along the eastern seaboard and Gulf of Mexico increased by 23 million people between 1960 and 2008, and continues to grow rapidly (Wilson & Fischetti, 2010).

The majority of current model projections of future tropical storms under many global warming scenarios project increases in intensity (wind speed, precipitation), inland penetration, and number of TCs (Li & Chakraborty, 2020). Recent research suggests that in response to anthropogenic warming there may also be a poleward expansion of the meteorological conditions favorable for TC formation. Under this scenario, even a modest shift in mean latitude where TC tracks form would significantly impact the storm landfall risk at higher latitudes (Studholme et al., 2022). There is considerable uncertainty though, over how such future storms will impact eastern North America as these models are hampered by gaps in the understanding of long-term trends and cycles in TC recurrence, intensity, and rate of change. Although the first efforts to develop a TC forecasting capacity had its beginnings in the 1870s, it was only in the post-WWII era that the modern instrumental record became established

Project Administration: R. Timothy Patterson

Resources: R. Timothy Patterson, Jennifer M. Galloway

Software: Nawaf A. Nasser, Eduard G. Reinhardt, Calder W. Patterson, Braden R. B. Gregory

Supervision: R. Timothy Patterson

Visualization: R. Timothy Patterson, Nawaf A. Nasser, Calder W. Patterson, Braden R. B. Gregory, Veronica Mazzella

Writing – original draft: R. Timothy Patterson

Writing – review & editing: R. Timothy Patterson

(Bradley, 2000; Knapp et al., 2010; Knutson et al., 2010; Oliva, Peros, et al., 2018; Sheets, 1990; Studholme et al., 2022). Some historical records in the WNAB extend back to the late fifteenth century but they generally only provide information on the most devastating TCs (Liu, 2004; Lockett, 2012; McWilliams, 1963). Without crucial baseline data that documents both the spatial and temporal distribution of large storms at centennial scales, it will be difficult to model the full spectrum of expected future events, including TCs that are rare but intense. There is thus urgency in this research as TCs were ranked as presenting the highest global risk at the 2019 World Economic Forum (Stockwell et al., 2020).

Since the first documented study of late Holocene hurricane records carried out at Oyster Pond, Massachusetts (Emery, 1969) research on TCs within the WNAB now encompasses a large body of work utilizing a wide array of geological and biological proxies (grain size data, organic content, X-ray fluorescence [XRF], geochemistry, and micropaleontology; e.g., Donnelly et al., 2001; Liu & Fearn, 1993; Oliva et al., 2017; Oliva, Peros, et al., 2018; Oliva, Viau, et al., 2018; D. J. Wallace et al., 2014; Winkler et al., 2020). There remain significant geographic gaps in TC research on the WNAB and only two previous studies have been carried out in Atlantic Canada (Oliva, Peros, et al., 2018; Yang et al., 2020). The vast majority of existing investigated TC records from lakes, ponds, lagoons, marshes, and so forth, in the immediate vicinity of coastal regions with only a few studies being carried out at inland locations (Oliva et al., 2017; Oliva, Peros, et al., 2018; Oliva, Viau, et al., 2018; Parris et al., 2010; D. J. Wallace et al., 2014). This has primarily been due to the difficulty in detecting paleotempest signals at inland locations using most conventional sedimentological techniques, where storm energy and impact become rapidly reduced (Patterson et al., 2020).

The passage of major storms, especially TCs, often significantly impacts sedimentation in lakes. Grain size analysis, which can be carried out quickly and cost-effectively, is a useful indicator of such depositional processes (Gammon et al., 2017; Oliva, Peros, et al., 2018; Parris et al., 2010; Yang et al., 2020). Any TC-induced paleotempest signals that become preserved in the lacustrine sedimentary record are generally characterized as spikes of coarser-grained sedimentation within finer sedimentary deposits and are principally derived from two distinct storm-related processes: (a) heavy precipitation that generally accompanies major storms often intensifies sediment erosion of the surrounding catchment resulting in runoff delivery of sediments to lakes (Cohen, 2003; Gallagher et al., 2016); and, (b) strong storm winds that result in the resuspension of finer deep lake sediments through a deepening of the wave base (Dean & Dalrymple, 1991; Hakanson & Jansson, 1983; Peng et al., 2005).

The development of end-member mixing analysis (EMMA) techniques for the analysis of grain size distributions now permits researchers to more precisely model the depositional signature (i.e., end members [EMs]) of specific catchment and lake hydrological processes (Dalton et al., 2018; Dietze & Dietze, 2019; Dietze et al., 2012; Macumber et al., 2018; Weltje and Prins, 2003, 2007). EMs are modeled by un-mixing multi-modal distributions that are comprised of the sum of many depositional processes, and the resultant EMs can then be associated with specific depositional processes (Macumber et al., 2018). With regard to the detection of storm signals, EMMA has been used to identify the sedimentary record of a particularly strong 1953 North Sea storm surge in a UK salt marsh on the UK Norfolk Coast (Swindles et al., 2018). Within the WNAB, Parris et al. (2010) used EMMA to identify several intervals of increased, storm-derived precipitation and paleo-flooding in the Holocene sedimentary record from several lakes in western Maine and New Hampshire. The use of EMMA also permits the recognition of more subtle grain size derived storm signatures than possible using conventional approaches, potentially opening up areas far removed from the coast, where storm energy becomes dissipated, for TC assessment. The recognition of TCs far removed from the coast provides the potential for such records to be correlated between lakes, which in turn may permit the reconstruction of paleostorm tracks. Such information would be of considerable value to researchers attempting to model the periodicity and distribution of future TCs in the WNAB and elsewhere.

Patterson et al. (2020) carried out a basin-wide EMMA analysis of the distribution of lake bottom sediments ($n = 100$) collected in 2015 from Harvey Lake, SW New Brunswick, >80 km inland from the Bay of Fundy, to determine whether the passage of the remnants of Hurricane Arthur, which as a sting jet enhanced post-tropical storm caused considerable damage to this inland area in July 2014 (Canadian Hurricane Centre, 2015). They observed an EM (very coarse silt, mode = 40 μm ; EM-40 μm) draping the lake bottom at all water depths, including areas >4.4 m water depth, which based on area historical wind speed data had been unimpacted by wave base remobilization since at least 1953. The widespread deposition of this EM in deeper water areas was attributed to fallout of storm wave base resuspended sediments from the water column in the wake of Arthur. Using a novel

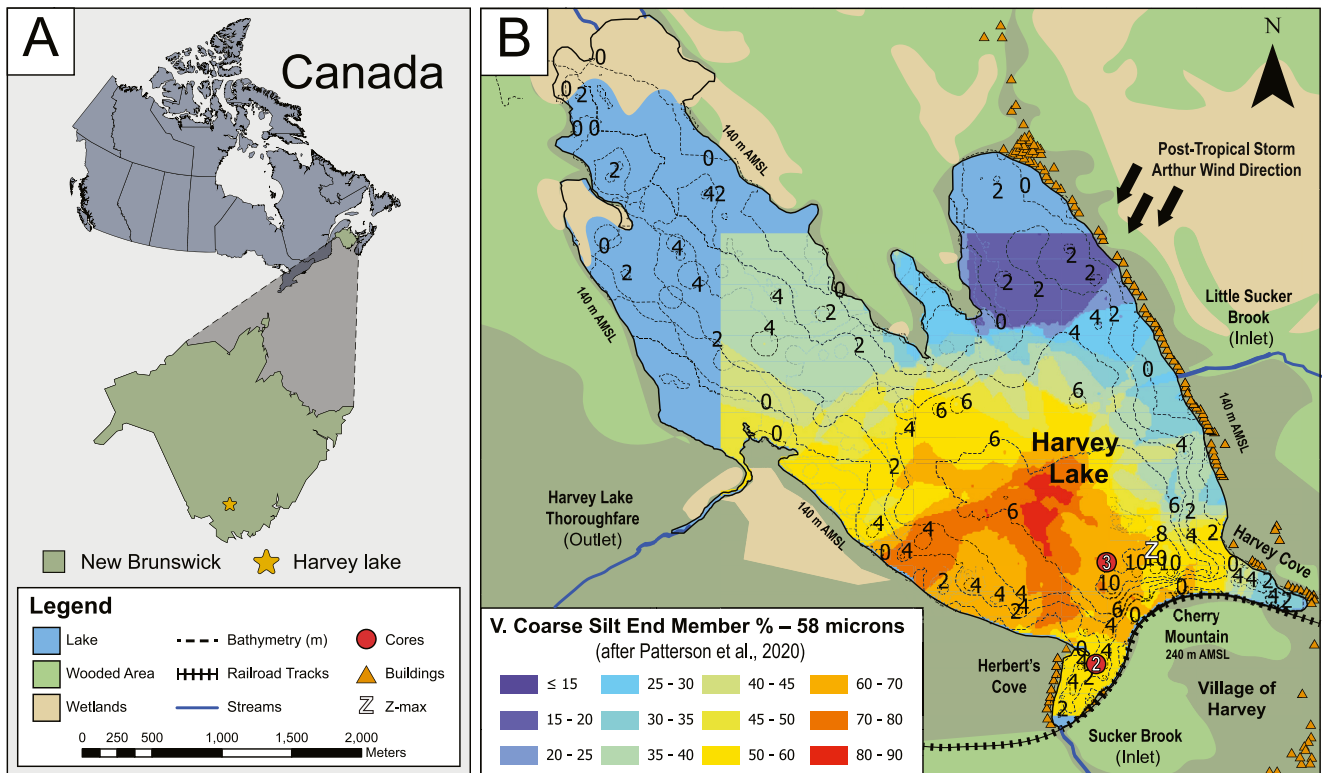


Figure 1. (a) Location of Harvey Lake within Canada and Province of New Brunswick. (b) An ArcGIS-generated map of Harvey Lake showing area physiography, core locations used in this research, lake bathymetry, elevation relative to meters above mean sea level for the lake shore and topographic high of Cherry Mountain, and the distribution of a coarse-grained end member determined to have been deposited in the wake of the passage of Post-Tropical Storm Arthur in July 2014.

geomatics method, they determined that the EM-40 μm was most concentrated in the SW and central part of the lake, particularly in an area NW of the ~ 11 m z-max, as well as in a sheltered 3–6 m deep cove in SW corner of the lake. The distribution of EM-40 in the lake was in agreement with the fetch length associated with the peak wind direction, strength, and duration during the passage of Arthur across the region (Figure 1).

Patterson et al. (2020) also carried out an ITRAX RF analysis of the same Harvey Lake bottom samples that were analyzed using EMMA. Through the past 20 years, XRF core scanners have proven to be a particularly useful and cost-effective tool for the interpretation of climatic and environmental change associated with parameters such as catchment weathering and productivity changes in paleolimnological records (e.g., Evans et al., 2021; Klamt et al., 2021; McNeill-Jewer et al., 2019; Oliva, Peros, et al., 2018; Roberts et al., 2016). Patterson et al. (2020) observed that the highest concentrations of the catchment runoff proxy Ti in the lake were in Herbert's Cove with focusing occurring within the nearby z-max (Figure 2). Based on the Harvey Lake EMMA and ITRAX results, they hypothesized that cores collected from either Herbert's Cove or the z-max would potentially yield the best paleostorm records archived in the lake.

As a follow-up to the recommendations made by the Patterson et al. (2020), multiproxy EMMA and ITRAX analyses were carried out on core subsamples from Harvey Lake. The purpose of this research is to: (a) test the hypothesis of Patterson et al. (2020) that TC records are archived in the sedimentary record of Harvey Lake; (b) determine if the modern distribution of TC EM-40 μm , deposited across the lake bottom during the passage of Post-Tropical Storm Arthur can be used as an analog of previous TC records in the lake sedimentary record; (c) determine using ITRAX analysis whether there have been any recognizable and distinct phases in the paleolimnological distribution of elements and elemental ratios that are associated with precipitation and runoff from the catchment; and (d) develop a method for reconstruction of TCs, their frequency, severity, and drivers of change.

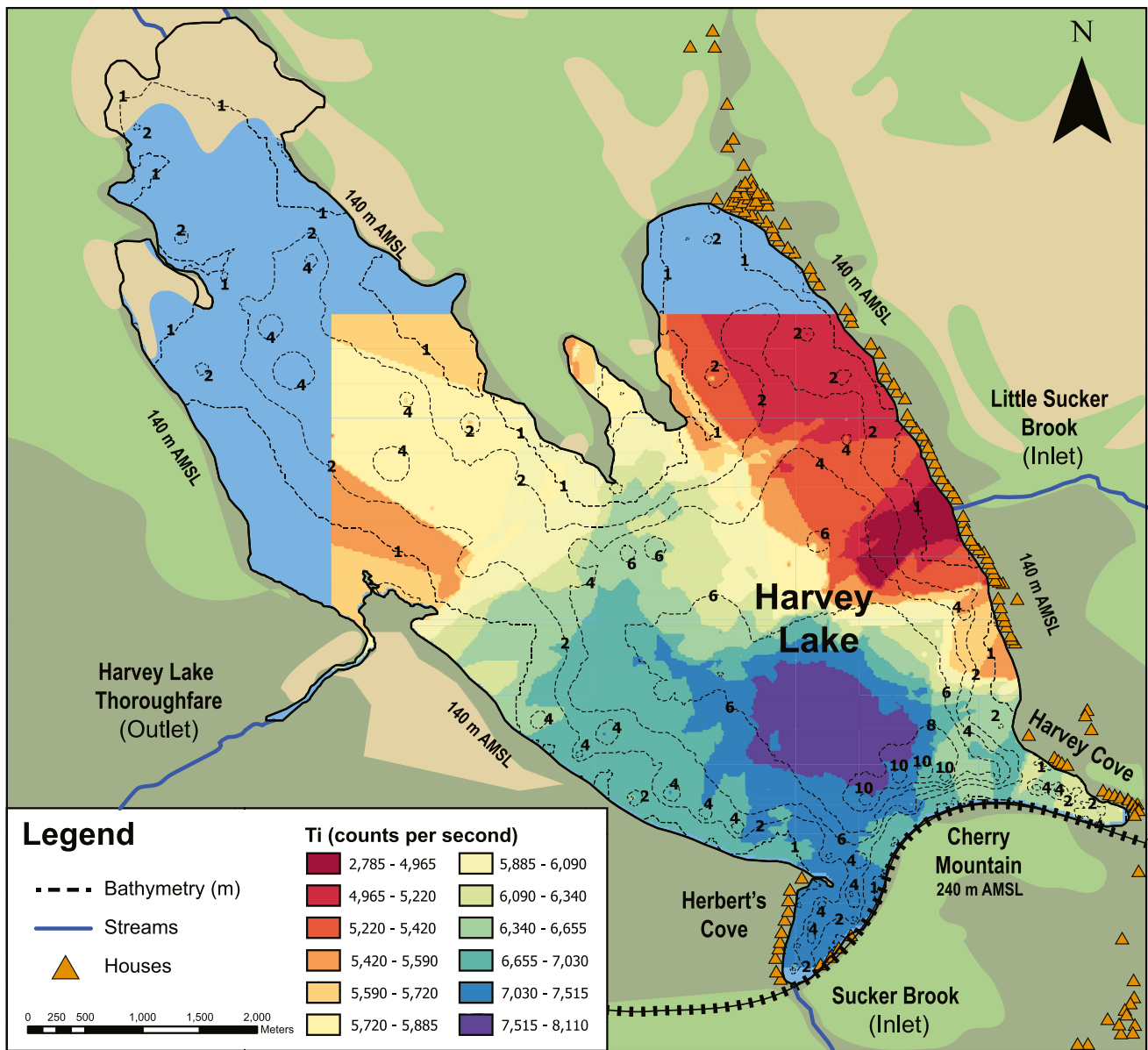


Figure 2. An ArcGIS-generated map of Harvey Lake showing area physiography, lake bathymetry, elevation relative to meters above mean sea level for the lake shore and topographic high of Cherry Mountain, and the spatial distribution of runoff through Sucker Brook derived Ti concentrations in counts per second (CPS) as calibrated from ITRAX XRF CS analysis results from analyzed sediment/water interface sample stations.

1.1. Impact of Post-Tropical Storm Arthur on Harvey Lake

In the research presented here, the EMMA signal left on the lake bottom of Harvey Lake that was derived from the passage of Post-Tropical Storm Arthur is used as an analog for the detection of down core records of TCs in the lake. As such, an overview of how and why Arthur impacted the lake is warranted to provide context on the intensity of storms required to leave such records. Hurricane Arthur developed from a non-tropical low over the southeastern United States that moved offshore and rapidly developed from a tropical depression to Tropical Storm Arthur on July 1, 2014 (NOAA, 2021). By July 4th, it had developed into a Category 2 hurricane before making landfall on North Carolina's Shackleford Banks where the storm began to weaken. Arthur subsequently began an extratropical transition, as it accelerated northeastward (Canadian Hurricane Centre, 2015). It tracked southeast of Cape Cod and as Post-Tropical Storm Arthur made landfall near Meteghan, Nova Scotia at 10:30 UTC on July 5th as a fierce storm with sustained winds estimated at 110 km/hr. The storm was unusual in that

it is uncommon for such a powerful storm to impact this region so early in the hurricane season. Of significance to this research is that the remnants of Arthur re-intensified as it crossed the Bay of Fundy and traversed New Brunswick with the development of a highly damaging sting jet with gusts of up to 130 km/hr over a broad geographic area along the storm's backside. In the area of Harvey Lake, rainfall totals at stations bracketing Harvey Lake in St. Stephen, NB and Gagetown, NB reported totals of 143 and 150 mm, respectively. At its peak, more than 52,000 power outages were reported in the region of the province around Harvey Lake, and efforts to repair the grid were prolonged due to storm damage. Many customers were still without power 10 days after the storm (Canadian Hurricane Centre, 2015). The high winds significantly impacted the lake as the deepened storm wave base resuspended deep-water sediments into the water column. During the peak of the storm, winds impacting Harvey Lake were primarily out of the NE which in combination with the fetch length resulted in lake bottom sediment reworking being most significant in the central and SW parts of the lake (Figure 1b). Due to the considerable storm wave base reworking of the lake bottom sediment, the entire lake water column turned brown and stayed that way for several days, a condition that had not been reported in living memory. In addition, there was also considerable catchment runoff related to the storm. The considerable volume of water that comprised the runoff associated with the storm is encapsulated in a statement provided by Harvey Lake Association (HLA) member Stephen Fox: "It (Arthur) took out our entire shoreline, primarily because the water rose so much and so rapidly. I remember that they had forecast the wind, but what no-one expected was the amount of rainfall" (Patterson et al., 2020). An assessment of Arcellinida (testate lobose amebae) obtained from sediment-water interface samples from throughout the Harvey Lake basin in 2015 indicated that Post-Tropical Storm Arthur also had a significant ecological impact. It was determined that the deepening of the wave base during the passage of the storm resulted in arcellinidans, a key intermediary trophic food web component, being carried into suspension along with very coarse silt grain particles and then redeposited at all water depths throughout the lake, forming exotic species assemblages (Atasiei et al., 2022).

1.2. Harvey Lake Physiography

Harvey Lake (45°43'45"N, -67°00'25"W) is a small temperate climate lake located adjacent and just north of the village of Harvey, York County, New Brunswick, Canada (Figure 1). The lake is relatively small with a surface area of 7.2 km² and a maximum depth of 11.8 m. The inlet streams are relatively small, with Little Sucker Brook entering the lake midway along the eastern margin of the lake and Sucker Brook flowing into the lake at the head of Herbert's Cove at the southwest corner of the lake (Figure 1). There is only one outlet stream, "The Harvey Lake Thoroughfare," which flows westward into nearby Second Harvey Lake. Cherry Mountain, located at the south end of the lake (45°43'38"N 67°00'59"W; 240 m elevation), is comprised of Late Devonian-Early Carboniferous Harvey Group rocks (Cherry Hill and Harvey Mountain formations; Pajari, 1973). The 75–100 m thick Harvey Mountain Formation sequence found there comprises laminated rhyolite lava flows, pyroclastic breccia, and ignimbrites intercalated with ash-fall tuffs (Dostal et al., 2016). Sucker Brook flows through forest and over outcrops of both the Harvey Mountain and Cherry Hill formations before entering Herbert's Cove in the southwest corner of the lake. Little Sucker Brook passes through agricultural land over Silurian metasedimentary basement rocks before entering the lake midway along the eastern margin of the lake (McKerrow & Ziegler, 1971).

2. Methods

2.1. Field Work

Two gravity Glew Maxi-cores were collected from Harvey Lake, New Brunswick in July 2017. A 250 mm core (HL-2017-GC-2; 45°43'42.535"N; 67°01'23.739"W) was collected from near the mouth of Herbert's Cove, Harvey Lake, New Brunswick at a water depth of 4.5 m and a second 230 mm core (HL-2017-GC-3; 45°44'11.252"N; 67°01'25.888"W) was collected from 7.5 m water depth just northwest of the lake z-max. The coring locations were documented using a Garmin GPSmap 76CSx GPS unit (± 5 m) but with a resolution improved to $\sim \pm 1$ m by sighting on-shore reference points (Figure 1). The cores were subsampled on-site at 2 mm resolution using a Glew core extruder (Glew et al., 2001), refrigerated, and transferred to Carleton University for subsequent analysis.

Table 1
Radiocarbon Dates for Bulk Samples From the Two Harvey Lake Cores, Calibrated With the IntCal20 Calibration Curve (Reimer et al., 2020) Following Conventions of Millard (2014)

	Lab ID	Depth (mm)	¹⁴ C age BP ± 1σ	Pretreatment	Cal BP ± 2σ
HL-2017-GC-02	UOC-8526	50–54	625 ± 24	Acid only	660–620 (37.7%) 612–653 (57.7%)
	UOC-8528	150–154	731 ± 31	Acid only	727–653 (95.4%)
	UOC-6358	165–170	721 ± 23	Acid only	692–655 (85.5%)
	UOC-8529	200–204	780 ± 24	Acid only	732–675 (95.4%)
	UOC-8530	240–244	751 ± 24	Acid only	727–666 (95.4%)
HL-2017-GC-03	UOC-8524	26–30	1,451 ± 32	Acid only	1,392–1,299 (95.4%)
	UOC-8521	60–64	1,154 ± 24	Acid only	1,175–1,043 (63.8%) 1,037–982 (31.6%)
	UOC-8522	116–120	2836 ± 24	Acid only	3,020–3,015 (0.5%) 3,005–2,863 (95.4%)
	UOC-8523	180–184	5827 ± 27	Acid only	6,728–6,556 (95.4%)

2.2. Laboratory and Data Analysis

2.2.1. Radiocarbon Dating and Age-Depth Modeling

To determine whether the cores were suitable for detailed stratigraphic analysis, radiocarbon dates were obtained at intervals in both cores. Bulk sediment samples (five from HL-2017-GC-2 and four from HL-2017-GC-3) were used for radiocarbon dating since macrofossils were absent and the sediment was homogeneous throughout both cores. All samples were radiocarbon dated by accelerator mass spectrometer at the Lalonde AMS Laboratory in Ottawa, Ontario, Canada. Samples were pretreated with a standard hydrochloric acid wash to remove carbonate material (Crann et al., 2017). Radiocarbon dates were calibrated based on the IntCal20 Northern Hemisphere terrestrial radiocarbon curve (Reimer et al., 2020) using the BACON package (Blaauw et al., 2020) for R Statistical Software (R Core Team, 2020; Table 1).

Core HL-2017-GC-3, collected from open water in the central part of the lake, was characterized by a series of relatively old radiocarbon dates with a basal radiocarbon date of ~6,600 Cal BP at 180–184 mm core depth, indicating a very low sediment accumulation rate of >70 years per 2 mm. As Harvey Lake is not stratified, with the lake bottom being well oxygenated at all depths (Atasiei et al., 2022; Patterson et al., 2020) it is likely that deposition of organic and inorganic sediments in the central part of the lake is being impacted by factors such as productivity, oxygen exposure time, and the activities of microbial decomposers (Sobek et al., 2009). At the sampling resolution possible using a Glew core extruder (2 mm), it was determined that it would be difficult to reliably discriminate individual paleo-storm events in such a low sedimentation rate environment so further analysis of this core was suspended.

Core HL-2017-GC-2, collected from Herbert's Cove, was characterized by a more typical basal radiocarbon date for a core collected from a mesotrophic temperature lake of this length (~700 Cal BP at 240–244 mm; Figure 3; Table 1). The core was divided into 29 equal thickness sections for generation of an age model. The age-depth model was generated using the R BACON package, which uses Monte Carlo simulations to estimate the best age model using the probability distribution of a given radiocarbon date, *a-priori* knowledge of the accumulation rate of the core, and a memory strength parameter that limits the variations in accumulation rate between a given depth interval and the previous interval based on a gamma distribution. The accumulation rate for Core HL-2017-GC-2 was assumed to be ca. 20 years/cm (acc.mean = 20, acc.shape = 1.5) and the gamma distribution had a mean value of 0.3 and a “strength” of 10, where the strength of the gamma distribution refers to the peak height said distribution (mem.mean = 0.3, mem.strength = 10). An inferred date of –67 cal yr. BP was placed at 0 cm depth to represent the age of sediments when the core was recovered in 2017. This correction was required as the year 0 in radiocarbon dating, and thus deemed to be the present, is 1950. This year was chosen to honor the publication of the first radiocarbon dates in December 1949 (Taylor, 1987, p. 97).

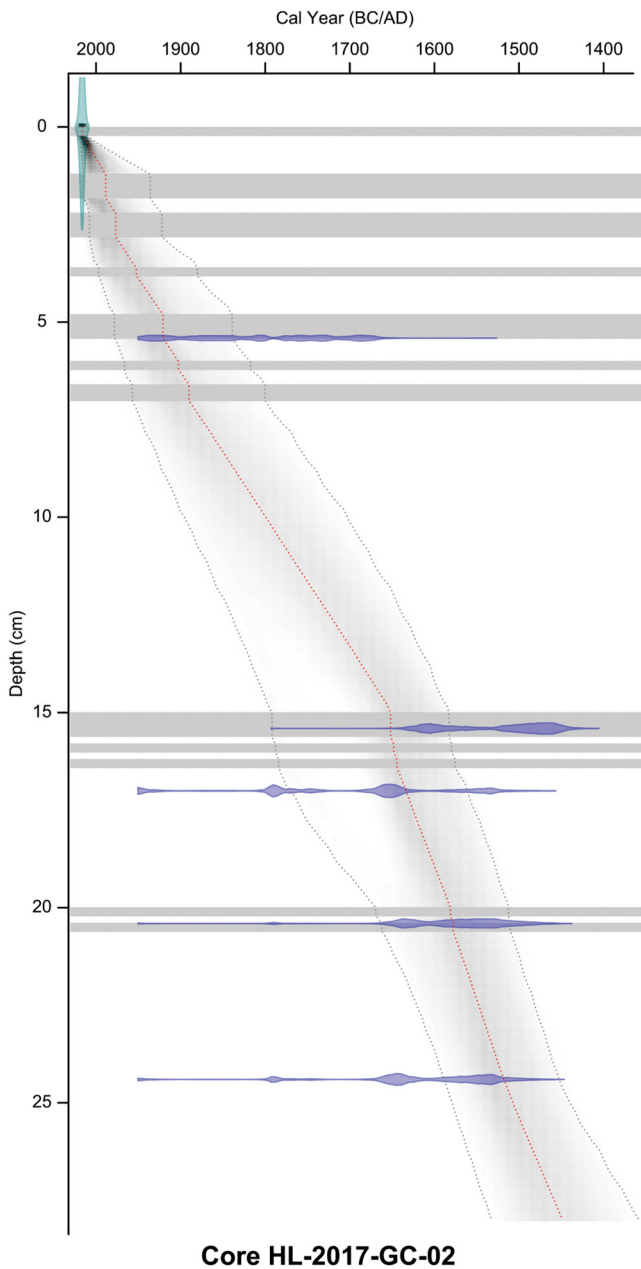


Figure 3. Age depth model for core HL-2017-GC-02 collected from Herbert's Cove. The model was created using the Bacon package (Blaauw et al., 2020) for R Statistical Software (Juggins, 2022) and the IntCal20 calibration curve (Reimer et al., 2020). To correct for “instantaneous” depositional events, the slump function within BACON was used to remove these sources of error. The core intervals associated with storm deposition were thus skipped during the calculation of the age model and are represented by 12 gray bands of varying thickness.

With regard to deposition for TC events in the core, it should be noted that they would have been deposited over at most 1–2 days. In contrast, a typical Bacon-generated age model assumes a relatively linear sedimentation rate. For sedimentary units up to several mm thick, this will result in a diachronous range in dates for what in reality are geologically instantaneous events (Patterson, 2022). To correct these “instantaneous” depositional events, the slump function within BACON was used to remove these sources of error. These storm-derived depositional units are represented by 12 gray bands of varying thickness.

2.2.2. Grain-Size Analysis

In preparation for grain-size analysis, the 115 sediment subsamples from core HL-2017-GC-2 (with sampling gaps at 0, 96, 170, 186, 190, 192, 212, and 214 mm) were processed at 2-mm-stratigraphic resolution using a protocol modified from Murray (2002) and van Hengstum et al. (2007). Briefly, 30% H₂O₂ was added to subsamples and then placed in an 80°C water bath to oxidize organic matter. Analysis of randomly selected samples treated using 10% HCl indicated that sediment carbonate content was insignificant so an HCl pretreatment was deemed unnecessary and not used. Following the H₂O₂ pretreatment, subsamples were analyzed using a Beckman Coulter LS 13 320 laser diffraction grain size analyzer equipped with a universal liquid module. Subsamples were hand agitated to suspend the sediments and then pipetted into the analyzer until an obscuration of $10 \pm 3\%$ was achieved. This slurry was then circulated within the module for 60 s before the first of three replicate runs. Each sample was analyzed in triplicate resulting in grain size distributions potentially ranging from 0.4 to 1500 μm . The triplicate analyses were averaged for each sample and Gradistat v8 was subsequently used to generate summary statistics for the grain-size distribution data (Blott & Kye, 2001). The grainsize data were used as inputs for subsequent EMMA, as described below.

2.2.3. End-Member Mixing Analysis

EMMA was carried out using the grain-size analysis results for the 115 subsamples obtained from Harvey Lake core HL-2017-GC-2 to characterize depositional processes influencing sedimentation in the lake. The EMMA analysis protocol followed that of Dietze et al. (2012) using R-Studio package EMMAgeo v.0.9.7 (Dietze & Dietze, 2019). Only robust EMs were considered, which were defined as those characterized by non-overlapping, interpretable EM loadings, with the addition of those where similar EM loadings occurred in most model runs (Dietze et al., 2012).

2.2.4. ITRAX XRF Analysis

Subsamples from the same core horizons used for the EMMA analysis were loaded into a custom-designed acrylic Sequential Sediment Reservoir (SSR) vessel using an inert laboratory spatula, evenly compacting the sediment to ensure no void spaces were present in the $\sim 0.5 \text{ cm}^3$ cuvette (modified after vessel described in Gregory et al., 2017). Each cuvette was sequentially analyzed using the Cr heavy element (Cr-HE) X-ray source (30 Kv, 28 mA, exp. time = 15 s, step-size 0.2 mm) on a Cox ITRAX $\mu\text{XRF-CS}$ at the

McMaster University Core Scanning Facility (MUCS). Twenty-five measurements from each sample reservoir were averaged and the standard deviation was calculated to document variability. Data are shown as total counts over the 15 s integration time. The individual elements generated through the XRF analysis were normalized for “matrix effects” using the Cr inc/Cr Coh scattering ratio (Chagué-Goff et al., 2016; Croudace et al., 2006; Gregory et al., 2019; Weltje et al., 2015).

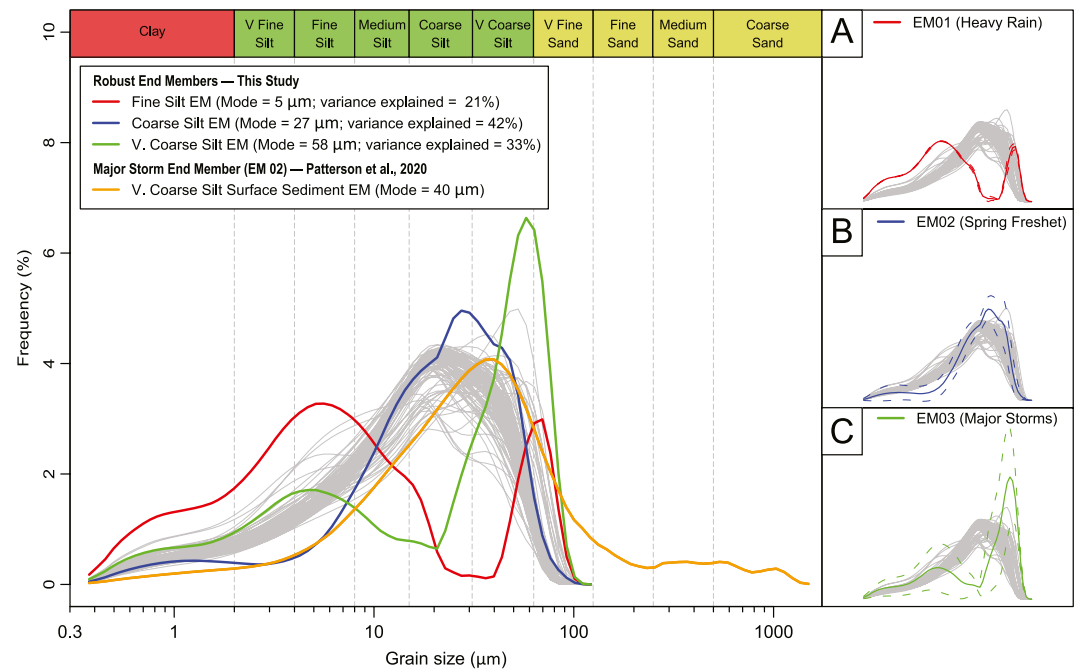


Figure 4. Grain size frequency distributions for the analyzed 115 subsamples (gray) from core HL-2017-GC-02, as well as the distribution of three derived robust end members (EMs) from the selected EMMA model that best explained the sediment grain distribution in the analyzed samples. For comparison, a major storm-derived EM (Post-Tropical Storm Arthur), which is widely distributed across the SW part of the modern Harvey Lake bottom is plotted as an overlay.

2.2.5. CONISS Cluster Analysis

Stratigraphically Constrained Incremental Sum of Squares (CONISS; Grimm, 1987) hierarchical cluster analysis in RStudio (Package: rioja; Juggins, 2022) was used to identify stratigraphic zones based on the raw EMMA and ITRAX-XRF data sets.

3. Results

3.1. End-Member Mixing Analysis

A total of 74 EMMA models were tested for core HL-2017-GC-2, which included a variable number of EMs ($q_{max} = 2-6$). These results collectively explained $80.8 \pm 5.8\%$ of the variance. The final selected EMMA model explained 78.6% of the variance and was comprised of three robust EMs (EM 01–03; Figure 4). In the context of EMMA, the term “robust” is a quantifiable value within EMMA analysis that measures variability in modeling EM grain size distributions; the greater the variability the less robust the EM (Dietze et al., 2014).

Of these three robust EMs, the fine silt EM 01 (mode = 5 μm , secondary mode = 60 μm , and variance explained = $\sim 21\%$) was periodically important below the 126 mm horizon in the core and was most prominent above the 72 mm interval in the core (Figures 4 and 5; Patterson, 2022). The coarse silt EM 02 (mode = 27 μm) explained $\sim 47\%$ of the observed variance and dominated the EM distribution throughout the entire core (Figures 4 and 5; Patterson, 2022). The very coarse silt EM 03 (mode = 58 μm , secondary mode = 6 μm) explained $\sim 33\%$ of the observed variance (Figure 4). This EM is characterized by a greater bimodal variation in comparison to EM 01 and EM 02. This EM was observed in 12 horizons in the core, and as with EM 01, became more abundant in sediments deposited above a core depth of 72 mm (Figures 3 and 5; Patterson, 2022).

3.2. Radiocarbon Age-Depth Modeling

The age model for core HL-2017-GC-2 spans the period from ~ 1490 CE at the base of the core (250 mm) to 2017 CE at 0 cm and was adjusted to account for 12 documented instantaneous storm-derived depositional events

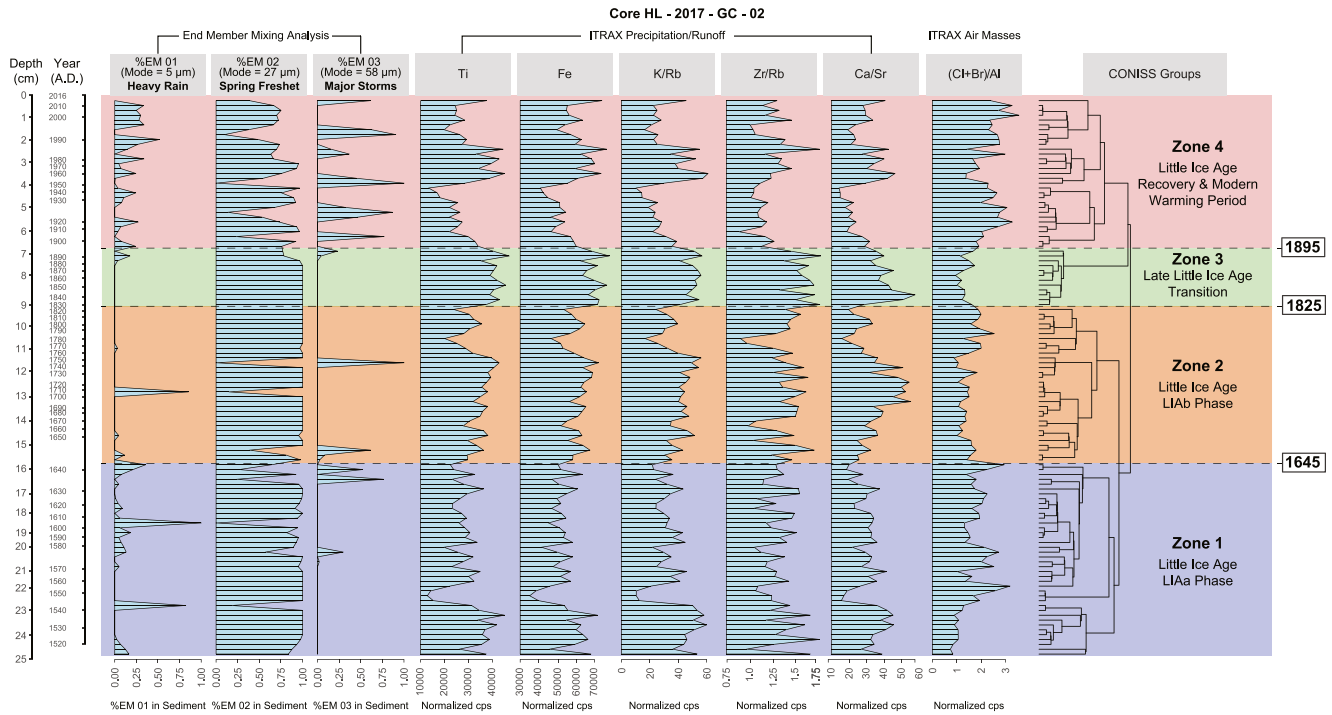


Figure 5. Down core relative distribution of the three identified end members in core HL-2017-GC-02, plotted against depth in core and Bacon age model estimated age for each sampled horizon. CONISS cluster analysis of EMMA and ITRAX data resulted in recognition of four distinctive zones in core record. Dashed horizontal lines delineate the relative occurrence rate of heavy precipitation events (EM01) and TC (EM03). Both results correlate well with phases of the Little Ice Age and subsequent development of the Modern Warm Era. Cross-hatched area spanning 0–2 mm in the core represents sediment lost during core subsampling.

(Figure 3). The age model indicates that there was a relatively consistent depositional rate, although a slight inflection at ~150 mm (mid-seventeenth century) indicates a subsequent slowing of the sedimentation rate.

With the exception of using the 2017 date of collection for the date at the top of the core, it was decided to not “lock in” any other calendar dates down core (e.g., EM peaks that might be linked to historically documented storm events). This was because the error range of radiocarbon dates and age model could potentially include multiple candidates for historically documented TCs. It is thus recommended that any future core analysis carried out in Harvey Lake, or any other lake in the region for that matter, also include additional ^{210}Pb and/or ^{137}Cs analyses. The resultant more detailed chronology for the post mid-nineteenth century interval will potentially not only permit the identification of specific storm events but also facilitate the correlation of events between lake basins. Such information is critical for the reconstruction of storm tracks for TCs from before the advent of instrumental data collection, when such information is often lacking.

3.3. Down Core XRF Element and Element Ratio Distribution

Although results for more than 50 elements were obtained during the ITRAX XRF analysis, only a subset of normalized element results (Fe and Ti) received further consideration. The criteria for element selection were related to previous research indicating that variability in their relative abundance could be related to intervals of enhanced or reduced catchment sedimentary runoff/weathering and hydroclimatic variability (Evans et al., 2021; Gregory et al., 2021; Gushulak et al., 2021; McNeil-Jewer et al., 2019; Oliva, Peros, et al., 2018; Roberts et al., 2016). In addition, four elemental ratios were calculated (Ca/Sr, Zr/Rb, K/Rb, and Cl + Br/Al) as these have been also demonstrated to be reflective of limnological processes associated with runoff, chemical weathering, grain size, and marine air mass influence (Chagué-Goff et al., 2016; Lo et al., 2017; Oliva, Peros, et al., 2018; Peros et al., 2017; Roberts et al., 2016).

The relative abundance of the other elements (Ti and Fe) and elemental ratios (Ca/Sr, Zr/Rb, and K/Rb) showed very similar patterns through the core, and all are associated with precipitation and associated runoff-driven sedimentary processes. It has been observed in many studies that increased relative abundance of the lithogenic

elements Ti and Fe are a proxy for high levels of precipitation and associated catchment erosion and in wash of clastic sediment (Gushulak et al., 2021; Oliva, Peros, et al., 2018; Roberts et al., 2016). It has also been suggested that the Zr/Rb ratio provides a proxy for grain size with lower values reflecting typically finer-grained clay size inwash and higher values reflecting the presence of medium to large silt-sized particles (Dypvik & Harris, 2001). With the exception of a significant dip in the values for these proxies beginning ~1540 and terminating by ~1560, there was little variability through the sixteenth and early seventeenth centuries. Beginning by ~1640, the measured values for this suite of proxies gradually increased until reaching a peak by ~1750 and then gradually declining again to a trough in the ~1780s. Another peak occurred by the 1830s, followed by another trough starting in the late nineteenth century. Values increased again reaching another peak by the 1950s. With the exception of the values for Ca/Sr that subsequently began a gentle decline that persisted until the 1950s, the other proxies maintained relatively stable values until the end of the nineteenth century before declining to the trough that coincided with the Ca/Sr trough. There was subsequently a rapid increase in the values for Ti, Ca/Sr, K/Rb, and to a lesser degree by Fe and Zr/Rb that peaked in the 1960s before declining again by the 1990s. Values for these proxies generally increased again thereafter with a notable peak for all save for Zr/Rb at the top of the core.

The relative abundance of Cl + Br/Al up core was generally out of phase with the element values and elemental ratios discussed above. In previous ITRAX core analysis studies, both Cl and Br have been associated with marine wash over or salt spray influences in coastal lakes, albeit considerably closer to the ocean than Harvey Lake (Chagué-Goff et al., 2016; Oliva, Peros, et al., 2018). Peros et al. (2017) attributed peak in Cl and Br in a core record from a flooded sinkhole in northern Cuba to increased evaporation associated with regional drying associated with the 8.2 kyr event. Tropical storm systems have also previously demonstrated to be responsible for major depositions of sea salt, of which Cl is a major contributing component to areas further inland (Mullaugh et al., 2013; Sakihama & Tokuyama, 2005; Zen et al., 2022). Values of this proxy increase from low levels at the base of the core to a major peak in ~1550, followed by an interval of relatively high levels in the 1570s and another significant peak around 1640. Measured values from ~1645 to 1825 were relatively stable and generally lower than measured during the sixteenth century. They continued to be relatively stable and lower still during the interval from ~1825 to 1895. Levels of Cl + Br/Al gradually increased to another high peak by about 1920, gradually declining to a trough in the 1950s. The relative abundance increased to high levels again after 1960 with high peaks measured in the early 21st century that had not been observed in the core since the sixteenth and early seventeenth centuries.

3.4. CONISS Dendrogram

Interpretation of the CONISS dendrogram (Figure 5) resulted in the identification of four distinct stratigraphical zones in the EMMA and ITRAX-XRF data sets: (a) Zone 1 (base of core and terminating at 15.8 cm [~1645]); (b) Zone 2 (15.6–9.2 cm; ~1645–1825); (c) Zone 3 (9.0–6.8 cm; ~1825–1895); (d) Zone 4 (6.6 cm to top of core; ~1895 to the time of core collection in 2017).

4. Discussion

4.1. End-Member Characterization

Core HL-2017-GC-2 was characterized by three robust EMs that explained a majority of the variance in the grain size data (Figure 3; Patterson, 2022). The fine silt EM01 (mode = 05 μm) that also features a very fine sand peak is hypothesized to be primarily derived from heavy rain events. Such events can occur in SW New Brunswick at any time of the year (Clair et al., 1994; El-Jabi et al., 2013), but in the core HL-2017-GC-2 record would have only been deposited during seasons when there was no winter ice cover. Coarser-grained sediment runoff (see description of EM02 below) is generally restricted to higher energy water flow associated with spring runoff. As spring progresses and the soil melts, the volume of runoff becomes much reduced due to infiltration, significantly limiting the capacity of the system to transport coarse-grained (silt-sand) sediments from the catchment into Harvey Lake. However, following an intense or prolonged rainfall event, the capacity of the soil to absorb water becomes overwhelmed and infiltration-excess overland flow can develop into sheet overland flow that would gush downslope, carrying both coarse and fine sediments into Harvey Lake. Based on a comparison of April–November rainfall events recorded at three successive Government of Canada Climate stations that existed in nearby Harvey Station from 1920 to 2004 (Patterson, 2022) and the occurrence of EM01 events through the

same time interval in the core (Figure 4) it is estimated that single or multi-day rainfall events of >110 mm were required to generate infiltration-excess overland flow into Herbert's Cove. This hypothesis is supported by experimental research where it was determined under a variety of slope regimes from 5% to 25% and rain intensities from 30 to 90 mm hr⁻¹ that the derived sediment was primarily in the 2–8 μm size range (Kiani-Harchegani et al., 2018). Following infrequent very heavy rainfall events, it is reported that the Sucker Brook outflow is very muddy, forming a plume that extends far out into the cove (Judy Little McNally and Anne Jamieson, Harvey Lake Associations and Herbert's Cove residents, personnel communication, 2022). It is thus likely that these infrequent runoff events with associated considerable suspended load are responsible for the deposition of EM01 at the core site.

The most abundant EM recognized in core HL-2017-GC-2 was the coarse silt EM02 (mode = 27 μm). We hypothesize that this EM provides a record of the yearly spring freshet flow from Sucker Brook into Herbert's Cove (Figure 1). In New Brunswick, and elsewhere throughout many northern latitude areas, discharge associated with the spring thaw is the most significant flood of the year, as water is released from the rapidly melting snowpack. This results in coarser allochthonous material being transported with runoff from the catchment (Government of New Brunswick Flood History Database, 2012; Macumber et al., 2018; Spence & Woo, 2008). In New Brunswick, this discharge progressively decreases as spring develops, as snow cover disappears and frozen soil thaws leading to increased infiltration of meltwater. This process gradually reduces the ability of snow meltwater to transport coarser-grained sediments within the entrained bed- and suspended load from catchments into lakes and streams, reaching a low point with the arrival of summer (Clair et al., 1994; El-Jabi et al., 2013). This interpretation of the genesis of EM02 is corroborated by the high concentration of Ti in lake bottom sediments throughout Herbert's Cove and the SW part of the Harvey Lake basin (Figure 2). Titanium is a lithogenic element and increased concentrations of this element are a proxy of catchment erosion and in wash of clastic sediment. In Harvey Lake, the Ti most likely originates from the breakdown of TiO₂ in Ilmenite, which is common in the volcanic deposits comprising the Harvey Group volcanic rocks of Cherry Mountain over which Sucker Brook flows. Entrained Ti flows through Sucker Brook into Herbert's Cove and on out into the lake where it becomes focused in the lake z-max (Patterson et al., 2020). Sucker Brook is, for most of the year, a very quiet stream with a rounded pebble/cobble paved bottom. Each year during spring, freshet water flow through the brook increases considerably and becomes visibly and darkly muddy with a visible plume extending one third of the way out into the cove, indicating that there is a considerable suspended load, which is most likely the primary source of the observed elevated Ti concentrations across the lake bottom and the dominance of EM02 downcore (Figure 2; Patterson et al., 2020).

The very coarse silt EM 03 (mode = 58 μm) is very similar to the very coarse silt previously observed in sediment-water interface samples collected in 2015, primarily from the central and southwest areas of Harvey Lake (EM-40 μm; Patterson et al., 2020, Figure 4). Patterson et al. (2020) reported that EM-40 μm was widely distributed across the lake basin, including areas of >4.4 m water depth, which had been unimpacted by wave base remobilization since at least 1953 when wind speed data became available. These researchers interpreted their EM-40 μm to be derived from the passage of Post-Tropical Storm Arthur across the area in 2014, the result of fall-out over the course of a few hours of resuspended sediments from the water column. This EM was most concentrated in the central and southwest part of the lake at >6 m water depth, as well as within the z-max (~11 m), and throughout Herbert's Cove (3–6 m), where core HL-2017-GC-2 was collected (Figure 1). Although the very coarse silt EM03 (mode = 58 μm) of this study and the very coarse silt EM-40 μm of Patterson et al. (2020) are not identical, we hypothesize that they are both of TC origin and comparable. This is because the modes of the four EMs derived by Patterson et al. (2020) for the entirety of the Harvey Lake basin included grain size distributions from Herbert's Cove that comprised only a small proportion of the entire data set, whereas EM03 of this study only includes modes derived from grain size distributions entirely restricted to the small geographic area of Herbert's Cove. In addition, EM03 of this study was observed in the core-top (2–4 mm) samples recovered from core HL-2017-GC-2, which aligns well with the wide distribution of the 2015 sediment-water interface distribution of EM-40 μm in Herbert's Cove (Figure 4). The age model for core HL-2017-GC-2 estimates an approximate age of CE 2011–2016 for the 2–4 mm depth in the core. It is more likely that EM03 from this interval represents sedimentary evidence of Hurricane Arthur, which passed over the lake as a powerful and damaging post-tropical storm on July 5, 2014, as opposed to the remnants of Hurricane Irene, which passed through the region as an extratropical cyclone on August 28, 2011. This is because Arthur generated very large wind waves that depressed the storm wave based and remobilized a considerable volume of lake bottom sediment into the

water column, which according to the Harvey Lake Association, turned the entire water column brown for several days (Patterson et al., 2020). In contrast, due to the prevailing winds associated with the storm, the passage of Irene had no observable physical impact on Harvey Lake and the surrounding area, making it unlikely that this storm deposited the observed coarse silt EM. This observation clearly indicates the significance of the relative position of a lake relative to the storm track and associated wind field in determining whether or not a record of a particular storm will be deposited on the lake bottom.

It is important to note that high rainfall events that generate muddy runoff into Herberts Cove and produce EM01 signatures are also a characteristic of TC events such as Arthur that also result in the lake water turning brown, but in these cases produce EM03 signatures (Patterson, 2022). The key difference between the high rainfall events that produce EM01 and the TCs that generate EM03 is that the latter are also associated with high winds that produce large waves. The deepened wave base results in the suspension of lake bottom sediments that mix in the water column with rainfall-derived sediments simultaneously washing into the lake from the catchment. When the rain stops and the winds subside, and the sediments in the water column fall out of suspension to the lake bottom, the resultant sediment drape forms EM03. In contrast, there is often very little wind associated with heavy rainfall events derived from slow-moving low-pressure systems that may have a continental origin out of the west (Clair et al., 1994; El-Jabi et al., 2013).

4.2. Paleo-Major Storm Event Record

Visual inspection of the EMMA results through the post-CE 1490 stratigraphy of Core HL-2017-GC-02 shows evidence of 12 preserved major storm occurrences including at the top of the core Post-Tropical Storm Arthur in 2014 (Figure 5). As discussed above, the predominant wind field direction associated with the passage of major storms would have influenced the deposition of storm-derived sediments at the Herbert's Cove coring site so records of many storms that traversed the region are undoubtedly not preserved. There is also a tradeoff in recording storm records between the rate of sedimentation derived from lake productivity, deposition derived from the yearly spring freshet and runoff associated with major rainfall events versus the periodicity of storm wave base reworking. It is conceivable that two major storms spaced closely in time with similar wind fields that might result in wave base reworking that would produce EM 03 records that are indistinguishable from each other. That said, the records of EM03 in the core roughly correspond to the record of intense rainfall events recorded by EM01 (Patterson, 2022). On this evidence, it is concluded that the storm deposition record observed in the core provides a reasonable coverage of major storms impacting the lake with wind fields that would have resulted in EM 03 deposition in Hebert's Cove. CONISS cluster analysis of the EMMA and ITRAX element and element ratio results produced a zonation indicative of four major phases of relative storminess and hydroclimate related to changes in lake water levels, weathering, and associated runoff from the catchment (Figure 5). The CONISS zonation corresponds with an interval of increased storm activity that occurred before ~1645 (Zone 1), followed by a major storm gap spanning the period ~1645 to ~1825 (Zone 2) and ~1825 to ~1895 (Zone 3). There was a dramatic increase in intense rain and large storm events recorded in the Harvey Lake record spanning the period ~1895 to the present (Zone 4). The CONISS-derived overall distribution of EMMA-derived great storms and intense rainfall events and ITRAX determined changes in precipitation and runoff in the Harvey Lake record provides evidence of major shifts in the regime of paleotempest events occurring on a centennial scale. The CONISS zonation correlates well with the visual inspection results of the EMMA data alone which would place the upper boundary of the lowermost stormy/heavy rain interval at slightly later in ~1650, rather than ~1645, and the base of the modern stormy/heavy rain interval at ~1890 rather than ~1895.

A comparison between the EM 03 and ITRAX results indicates little direct correlation between individual major storm events and a specific element or element ratio spikes. This suggests that although the general pattern of major storm periodicity and the hydroclimatic regime influencing the Harvey Lake basin were in confluence through the past ~520 years, runoff events related to specific major storms, as recorded by the ITRAX data, were of less importance in recording individual storms events than wind fetch related storm wave base lake bottom sediment reworking. As discussed in Section 4.1 above in the context of EM 02, spring runoff significantly influences lake water budgets and sediment runoff throughout the region. The ITRAX results, as demonstrated by the modern distribution of lake bottom Ti in the lake (Patterson et al., 2020; Figure 2), seem to be primarily recording more localized climate variability through decadal-scale changes in runoff intensity to the lake through Sucker Brook during the spring freshet. These cycles of increase and subsequent decline in relative Ti, Ca/Sr,

Fe, and K/Rb values are discernible throughout the core record (Figure 5). Precipitation and temperature in this region are controlled by the complex interaction of multiple teleconnections (Patterson & Swindles, 2015; Walsh & Patterson 2022a, 2022b) including; the Atlantic Multidecadal Oscillation (AMO; Ruiz-Barradas et al., 2013; Alexander et al., 2014), Pacific Decadal Oscillation (PDO; Mantua & Hare, 2002), North Atlantic Oscillation/Arctic Oscillation (NAO/AO; Olsen et al., 2012; Li et al., 2017), El Niño-Southern Oscillation (ENSO; Hu & Feng, 2012), Schwabe Solar Cycle (SSC; Hathaway, 2015), and Quasi-Biennial Oscillation (Gray et al., 2018). For example, the AMO is characterized by a multidecadal variability of sea surface temperatures in North Atlantic Ocean surface waters. During an AMO + warm phase, eastern North America is characterized by increased temperatures, decreased precipitation, and greater drought probability (Alexander et al., 2014; Lyu & Yu, 2017).

4.3. Harvey Lake Within the Context of the West North Atlantic Basin

The cluster of numerous heavy rain (EM01) events and significant storm records (EM03) deposited before ~CE1650 in the Harvey Lake core, correlates with a well-documented pattern of heightened hurricane occurrences throughout the WNAB spanning from CE1400 to ~1650–1675 (e.g., southern New England salt marshes [van de Plassche et al., 2006]; Mattapoisett Marsh, MA [Boldt et al., 2010]; Outer Banks, NC [Mallinson et al., 2011]; Salt Pond, MA [Donnelly et al., 2015]; Thatchpoint Bluehole, Bahamas [van Hengstum et al., 2013]; Robinson Lake, NS [Oliva, Peros, et al., 2018]). For the Harvey Lake record, CONISS analysis of the EMMA data alone results in a major zonal break occurring at ~1650, whereas inclusion of runoff, precipitation, and air mass indicator ITRAX data results in the CONISS determined break occurring very slightly earlier at ~1645 as delineated by Zone 1 in Figure 5. It has been hypothesized that the high number of major storms recorded throughout this interval was related to an increase in Atlantic Meridional Overturning Circulation (AMOC) in combination with a southward shift of the Intertropical Convergence Zone as the Northern Hemisphere began to cool at the beginning of the Little Ice Age (LIA), which spanned the thirteenth to nineteenth centuries (Jones et al., 2021; Lamb, 1995). The LIA was characterized by wide-scale climate deterioration and the lowest global temperatures of the entire Holocene (Marcott et al., 2013; Matthews & Briffa, 2005). The LIA in the North Atlantic region has been divided into two cold periods. The initial phase is often referred to as the Medieval Cold Period, or LIAa, and ended by 1650 (Maslin et al., 2019), which correlates well with the early phase of major rainfall and major storms elsewhere in the WNAB, as well as in the Harvey Lake record. The deterioration in climate associated with the onset of LIAa was instrumental in extinguishing the Norse colonies on Greenland, and led to famine, wars, social unrest, and migrations in Europe (e.g., Fagan, 2001; Jones et al., 2021; Lamb, 1995; Parker, 2018). For example, the decades of the well-documented Grindewald Fluctuations, which took place during this interval, were characterized by some of the worst weather of the entire millennium throughout the northern Hemisphere (Jones et al., 2021; Parker, 2018). Of direct significance to the Harvey Lake storm record, atmosphere-ocean circulation changes related to the development of the LIAa may have led to an increase in Florida Current transport and flow intensity within the Gulf Stream (Lund et al., 2006), which would have resulted in a rapid increase in sea surface temperatures along the east coast of North America (e.g., 2°C increase in the Gulf of Maine, Wanamaker et al., 2008; Chesapeake Bay, Cronin et al., 2010; warmer SSTs in the Sargasso Sea and Bermuda Rise, Keigwin, 1996). As warm water conditions are amongst the most important factors controlling major development and track, higher SSTs particularly in the Gulf of Maine would have provided a conduit for storms to track toward Harvey Lake in SW NB.

Additional evidence of increased storminess across SW New Brunswick through the LIAa phase of deposition is provided by major peaks and generally elevated levels of Cl + Br/Al in the Harvey Lake core. Both Cl and Br derived from ITRAX have previously been used to assess marine influence over time in coastal lakes (Chagué-Goff et al., 2016; Oliva, Peros, et al., 2018). In addition, multiple studies have been carried out assessing the importance of major tropical storms delivering Cl derived from surficial ocean waters to the land through rainfall (Mullaugh et al., 2013; Sakihama & Tokuyama, 2005; Zeng et al., 2022). It has also been determined that the associated rain volume, wind speed, and wind direction significantly influence the concentration of Cl wet deposition in a region (Mullaugh et al., 2013). At the decadal-centennial scale under assessment in core HL-2017-GC-2, changes in the nature and provenance of air masses influencing the area will also influence the observed Br and Cl concentrations (Oliva, Peros, et al., 2018). Although previous research on the importance of these signatures has been limited to coastal areas and not a location such as Harvey Lake >80 km inland, it should be noted that many major tropical storm systems are often 100s of km across and rainbands of precipitation

associated with these storms can easily extend from far off shore to far inland (Skwira et al., 2005). In addition, to the best of our knowledge, this variable has not previously been assessed in an inland lake.

The near disappearance of intense rain events and TCs in the interval spanning from ~1645 to 1825 in the Harvey Lake record (zones 2 and 3) corresponds to a second and more intense phase of LIA conditions (LIAb) in the region (Lamb, 1995; Oliva, Peros, et al., 2018) that resulted in colder Northwest Atlantic SSTs and a redirection of TC tracks (Mann et al., 2009; Saenger et al., 2009) as well as a transitional Late Little Ice Age Zone 3 (~1825–1895; Figure 5). Of significance, CONISS analysis carried out on the EM and ITRAX analysis data, excluding the Cl + Br/Al data, results in a clustering where the LIAb phase terminated in 1895 at the Harvey Lake site. Including this marine air mass measure, as shown in Figure 5, results in the formation of a transitional ~1825–1895 Zone 3. Zone 3 is characterized by increased abundances of proxies associated with increased runoff, and related grain size/chemical weathering (Fe, Ti, Ca/Sr, Zr/Rb, and K/Rb), but in the absence of major storm and rainfall events. In this area, the hypothesis that best explains such a scenario is the presence of heavy winter snowfalls that would lead during the subsequent spring freshet to an increase in sediment input to the lake through Sucker Brook. The absence of major tropical storm influence during this phase is corroborated by the very low relative levels of Cl + Br/Al through the Zone 3 interval.

The period in the core record of Harvey Lake spanning ~1895 to the present (Zone 4) is characterized by the highest concentration of heavy rainfall and TCs in the entire >500 years sedimentary record (Figure 5). The levels of Cl + Br/Al through the Zone 4 interval are also amongst the highest of the entire record indicating an enhanced marine air mass influence across the region. This corresponds with the gradual ending of the LIA in the late nineteenth century and to a general SST warming in the WNAB. Sedimentary records of an increase in TCs during this interval have also been found elsewhere at several sites through the WNAB (e.g., Thatchport, Bahamas, van Hengstum et al., 2013; Mattapoisett Marsh, MA, Boldt et al., 2010; Lighthouse Bluehole, Belize, Denommee et al., 2014). Multiproxy analysis (oxygen, nitrogen, and radiocarbon isotopes) carried out in the Gulf of Maine indicates that there was a significant SST warming there that commenced in the late nineteenth century (2.2°C per century), as the LIA came to an end (Whitney et al., 2022). This increase in temperature has been linked to a renewed weakening of the AMOC, as hypothesized to have occurred during LIAa, that would have forced the Gulf Stream to a position closer to the Gulf of Maine (Thibodeau et al., 2018; Zhang & Vallis, 2007). Warmer water conditions in the Gulf of Maine, with possibly the highest SSTs recorded there during the past 1,000 years (Whitney et al., 2022), would have provided a conduit for storms to track into southern NB. In contrast, other researchers have concluded that the AMOC was not significantly altered during the LIA. They conclude that the observed hydroclimatic impacts were instead related to changes in wind regime (e.g., Moreno-Chamarro et al., 2015; Moreno-Chamarro, Ortega, et al., 2017; Moreno-Chamarro, Zanchettin, Lohmann, & Jungclaus, 2017; Moreno-Chamarro, Zanchettin, Lohmann, Luterbacher, et al., 2017; Thirumalai et al., 2018).

In a recent cross-wavelet time series analysis of annual spring ice-out dates in this region (spanning 1876–2020, including Harvey Lake), against teleconnections known to influence climate in the region, it was found that there was also a major shift in ice-out patterns starting in ~1895 as the LIA waned and the modern warm era began (Patterson Swindles, 2015; Walsh & Patterson, 2022a). This late nineteenth century shift correlates strongly with the initiation of increased storminess in the Harvey Lake record and throughout the WNAB. It also correlates with the increased influence of marine air masses in the Harvey Lake core record. Walsh and Patterson (2022a) determined that amongst several instrumental climate teleconnections assessed, shifts in the influence of the SSC and PDO were particularly influential in the development of ice-out conditions that have prevailed since the onset of the modern warm era. In an analysis of post-1890 instrumental records, Walsh and Patterson (2022b) determined that the dominant climatic driver of extreme weather throughout eastern North America was the SSC, which exhibited a long-standing, stationary relationship with all extreme instrumental precipitation records studied. The reason for this association is the fundamental linkage between the SSC and Total Solar Irradiance (TSI), which through amplifiers significantly influences atmospheric, oceanic, and terrestrial heating and circulation (Gray et al., 2010; Kopp, 2014). The observed coeval correlation between the climate shift observed in the ice out/instrumental climatic record and the increase in storminess and influence of marine air masses beginning in the mid-1890s is probably not coincidental.

A late nineteenth and onward increase in TCs is not recorded at all sites through the WNAB though, including Robinson Lake in Nova Scotia (Oliva, Peros, et al., 2018). It has been suggested that the lack of a coherent pattern

of TC events across the region during the recovery from the LIA and into the modern warm era may be a reflection of the stochastic nature of hurricane landfalls (Donnelly et al., 2015; E. J. Wallace et al., 2020). Further, retrospective attribution of specific TCs may sometimes be difficult as storms may impact different lakes in different ways (Kuha et al., 2016) depending on the relative distance of lakes from the eye of a storm, and associated wind field (Donnelly et al., 2015; D. J. Wallace et al., 2014). For example, both hurricanes Juan (September 2003 – Category 2 at landfall) and Dorian (September 2019, Category 2 offshore and strong post-tropical at landfall) caused significant damage in Nova Scotia, but had no impact on the area of Harvey Lake, 400 km away in SW NB.

From the perspective of potentially attributing downcore occurrences of storm records in Herbert's Cove, the prevailing wind direction during the transit of major storms would have played an important role in preserving evidence of these storms. During the passage of Arthur, as discussed in detail in Section 1.1, the strongest winds were from the NE resulting in fetch conditions that enhanced sediment accumulation in the SW part of the lake, including Herbert's Cove (Figure 1a). If the wind field during the passage of Arthur had been from a different direction, sediment accumulation in Herbert's Cove might have been significantly reduced. For example, despite the significant impact of Arthur on Harvey Lake, there is little sedimentological evidence of passage of the storm in the NE quadrant of the lake where the fetch was minimal (Figure 1a). There are undoubtedly multiple major storms that have impacted the region over time that due to the wind field associated with their passage have left little impact on the sedimentological record recorded in the Herbert's Cove core. A good example would be Tropical Storm Bob that tracked NW of Harvey Lake in 1991 with a wind field that was from the SW as it tracked past. Discussions by the authors with long-time local residents during fieldwork in the area confirmed that the storm had little noticeable impact on the lake.

5. Summary and Conclusions

This study presents a 2-mm-resolution analysis of TC and high rainfall events preserved in a core record spanning the last ~520 years from Harvey Lake, SW New Brunswick, Canada. This analysis, only the second to be carried out in Atlantic Canada (after Oliva, Peros, et al., 2018; Oliva, Viau, et al., 2018), is unique in that it is the first assessment of TC records in the WNAB to be carried out on an inland lake; in this instance >80 km from the coast (Oliva, Viau, et al., 2018). Sedimentological analysis of major storm events in coastal lake and lagoon core records generally relies on visual recognition of coarse sediment layers derived from storm-derived overwash (Oliva et al., 2017; D. J. Wallace et al., 2014). Away from the coast, especially at inland locations, where the energy of storm events is attenuated, such records do not form. EMMA carried out on the sedimentary record of the Harvey Lake core permitted recognition of three robust EM signatures, formed as a result of distinct depositional drivers (Figures 4 and 5). EM 01 (mode = 5 μm , secondary mode = 60 μm) is interpreted to be derived from major rainfall events of >100 mm where the infiltration capacity of the catchment is overwhelmed and both coarse and fine sediments are washed into the lake basin. Coarse silt dominated EM02 (mode = 27 μm) dominated the sedimentary record and is interpreted to have been deposited during the spring freshet when rapid snow melt resulted in significant catchment erosion of coarser allochthonous sediment into the lake. This interpretation is corroborated by the distribution of runoff-derived Ti in Herbert's Cove that is transported into the lake through Sucker Brook, primarily during Spring Freshet (Figure 2). The very coarse bimodal EM 03 (mode = 58 μm , secondary mode = 6 μm) occurred episodically in the core (Figure 5). Based on comparison with EMMA sediments deposited at the sediment-water interface during the 2014 passage of Post-Tropical Storm Arthur (Patterson et al., 2020), EM03 is interpreted to be derived from the influence of similar storms.

The distribution of a number of EM01 and several EM03 events characterize an interval of increased heavy rains and TCs in this region from the beginning of the sedimentary record at the beginning of the sixteenth century to about 1650, which coincides with the early LIAa phase of the LIA (Maslin et al., 2019). Similar records of greater storminess have been recorded throughout the entire WNAB, likely related to the development of warmer coastal waters. The increase in SST in the nearby Gulf of Maine has been hypothesized to have been driven by a weakening of the AMOC, which would have forced warm water of the Gulf Stream closer to the coast. Such a shift would have provided a means for a greater number of major storms to obtain the warm-water fuel required for them to track up the eastern seaboard of North America and into the Maritimes (Donnelly et al., 2015; Oliva, Peros, et al., 2018). A visual inspection of the EMMA results correlates very well with a CONISS cluster analysis of both the EMMA and ITRAX proxies of runoff/weathering/precipitation (Mg, Ti, Fe, Ca/Sr, Zr/Rb, and K/Rb), which places the transition only slightly earlier in the core record at ~1645. The results are further enhanced by

the inclusion of ITRAX-derived Br and Cl data which provides documentation of the relative influence of marine air masses and associated major storm tracks off the ocean. In the Harvey Lake core record, this interval was followed by a period spanning from ~1645 to 1895 when heavy rain events and TCs nearly completely disappeared. Exclusion of the Br + Cl/Al data from the CONISS analysis resulted in the extension of the LIAb Zone to ~1895, whereas inclusion of the marine air mass proxy resulted in the formation of an ~1825–1895 Late Little Ice Age Transitional Zone 3 (Figure 5). The LIAb interval coincided with the coldest phase of the LIA, which corresponded with colder SST in the Northwest Atlantic (Mann et al., 2009; Maslin et al., 2019; Saenger et al., 2009). After 1845, there was renewed development of a large number of intense heavy rain and deposition of seven distinct TC in the Harvey Lake record during Zone 4, as the LIA came to an end and the current Modern Warm Period developed. This shift in TC tracks was, as had occurred during LIAa, may have been heavily influenced by a weakening of the AMOC and resultant coastward shift of the Gulf Stream. The ensuing warming of SSTs in the Gulf of Maine, that are at present the warmest that they have been in 1,000 years (Whitney et al., 2022), would have made it easier for TCs to track into SW NB. A concomitant increase in TSI that influenced an increase in the periodicity of extreme precipitation events in eastern North America (Walsh & Patterson, 2022b) may also have contributed to the increased occurrence of heavy rainfall events recorded in the Harvey Lake record after 1895. It should be noted though that determining the underlying causes for phases of the LIA is an area of active investigation with other research suggesting that an increase in TSI may not have significantly influenced the LIA (e.g., Chiodo et al., 2019; Neukom et al., 2019; Schurer et al., 2013). Further, there is contradictory research that suggests that the AMOC (and deepwater formation) may not necessarily have been altered during the LIA, but rather that the observed hydroclimate impacts occurred due to Atlantic-wide surface-circulation changes related to changes in the wind regime (e.g., Moreno-Chamarro et al., 2015; Moreno-Chamarro, Ortega, et al., 2017; Moreno-Chamarro, Zanchettin, Lohmann, & Jungclaus, 2017; Moreno-Chamarro, Zanchettin, Lohmann, Luterbacher, et al., 2017; Thirumalai et al., 2018). Whatever the underlying causes for the LIA, the Harvey Lake core record presents evidence that there was considerable variability in runoff during this turbulent climatic interval and the Br + Cl/Al data indicates a strong marine air mass influence across the region.

The results of this research indicate that EMMA is an important tool to recognize subtle records of high precipitation runoff events and TC-driven storm resuspension/runoff events in inland lakes where recognition of these phenomena would be impossible using conventional grain size analysis and sedimentological techniques. This reconnaissance analysis provides evidence that a similar approach carried out on other inland lake records elsewhere will permit a better understanding of how storm activity has shifted over time. The ITRAX analysis data provides important complimentary corroborating information on the nature of precipitation, runoff, and air mass movements across the region during the interval of deposition. These more detailed data can then be used to inform climate modelers, policymakers, and planners as they attempt to determine the distribution and periodicity of future TCs in the WNAB.

Acknowledgments

This work was supported by NSERC Discovery (#RGPIN05329), NRCan Clean Technology (#CGP-17-0704), and Carleton University Multidisciplinary Research Catalyst Fund (#187536) grants to RTP. The authors thank Jochen Schroer of NATECH Environmental Services for providing the baseline Bathymetry Map. The authors are grateful for the contributions of Dr. Sheryl Bartlett, chairperson New Brunswick Alliance of Lake Associations and past chairperson of the Harvey Lake Association for facilitating the research on Harvey Lake, as well as HLA member Jack Goode, for assistance with core collection. The authors appreciate the input provided by Jim Abraham of Environment Canada (retired) in assessing the likely impact of the Saxby Gale on SW NB. The authors also thank Dr. Elizabeth Anderson for helpful comments on an earlier draft of the manuscript. This work is a contribution to IGCP Project 725 "Forecasting Coastal Change."

Data Availability Statement

The underlying particle size data used for this research, upon which the derived EMMA analysis presented here is based, is archived in the Dryad data repository (Patterson, 2022).

References

- Alexander, M. A., Kilbourne, K. H., & Nye, J. A. (2014). Climate variability during warm and cold phases of the Atlantic Multidecadal Oscillation (AMO) 1871–2008. *Journal of Marine Systems*, 133, 14–26. <https://doi.org/10.1016/j.jmarsys.2013.07.017>
- Atasiei, D., Nasser, N. A., Patterson, C. W., Wen, A., Patterson, R. T., Galloway, J. M., & Roe, H. M. (2022). Impact of Post-Tropical Storm Arthur on benthic Arcellinida assemblage dynamics in Harvey Lake, New Brunswick, Canada. *Hydrobiologia*, 849(13), 3041–3059. <https://doi.org/10.1007/s10750-022-04912-x>
- Blaauw, M., Christen, J. A., Aquino Lopez, M. A., Esquivel Vazquez, J., Gonzalez, V. O. M., Belding, T., et al. (2020). rbacon: Age-depth modeling using Bayesian Statistics. R package v., 2.5.0. Retrieved from <https://CRAN.R-project.org/package=rbacon>
- Blott, S. J., & Kye, K. (2001). GRADISTAT: A grain size distribution and statistics package for the analysis of unconsolidated sediments. *Earth Surface Processes and Landforms*, 26, 1237–1248. <https://doi.org/10.1002/esp.261>
- Boldt, K. V., Lane, P., Woodruff, J. D., & Donnelly, J. P. (2010). Calibrating a sedimentary record of overwash from Southeastern New England using modeled historic hurricane surges. *Marine Geology*, 275(1), 127–139. <https://doi.org/10.1016/j.margeo.2010.05.002>
- Bradley, R. S. (2000). Past global changes and their significance for the future. *Quaternary Science Reviews*, 19(1–5), 391–402. [https://doi.org/10.1016/S0277-3791\(99\)00071-2](https://doi.org/10.1016/S0277-3791(99)00071-2)
- Canadian Hurricane Centre. (2015). *2014 Tropical cyclone season summary*. Canadian Hurricane Centre, Meteorological Service of Canada, Environment Canada document En55-8E-PDF, 20 p.

- Chagué-Goff, C., Chan, J. C. H., Goff, J., & Gadd, P. (2016). Late Holocene record of environmental changes, cyclones and tsunamis in a coastal lake, Mangaia, Cook Islands. *Island Arc*, 25, 333–349.
- Chiodo, G., Oehrlin, J., Polvani, L. M., Fyfe, J. C., & Smith, A. K. (2019). Insignificant influence of the 11-year solar cycle on the North Atlantic Oscillation. *Nature Geoscience*, 12(2), 94–99. <https://doi.org/10.1038/s41561-018-0293-3>
- Clair, T. A., Pollock, T. L., & Ehrman, J. M. (1994). Exports of carbon and nitrogen from river basins in Canada's Atlantic Provinces. *Global Biogeochemical Cycles*, 8, 441–450. <https://doi.org/10.1029/94gb02311>
- Cohen, A. S. (2003). *Paleolimnology: The history and evolution of lake systems* (p. 525). Oxford University Press.
- Crann, C. A., Murseli, S., St-Jean, G., Zhao, X., Clark, I. D., & Kieser, W. E. (2017). First status report on radiocarbon sample preparation techniques at the AE Lalonde AMS Laboratory (Ottawa, Canada). *Radiocarbon*, 59(3), 695–704. <https://doi.org/10.1017/rdc.2016.55>
- Cronin, T. M., Hayo, K., Thunell, R. C., Dwyer, G. S., Saenger, C., & Willard, D. A. (2010). The medieval climate anomaly and Little Ice Age in Chesapeake Bay and the North Atlantic Ocean. *Palaeogeography, Palaeoclimatology, Palaeoecology*, 297, 299–310. <https://doi.org/10.1016/j.palaeo.2010.08.009>
- Croudace, I. W., Rindby, A., & Rothwell, R. G. (2006). ITRAX: Description and evaluation of a new multi-function X-ray core scanner. *Geological Society, London, Special Publications*, 267(1), 51–63. <https://doi.org/10.1144/gsl.sp.2006.267.01.04>
- Dalton, A. S., Patterson, R. T., Roe, H. M., Macumber, A. L., Swindles, G. T., Galloway, J. M., et al. (2018). Late Holocene climatic variability in Subarctic Canada: Insights from a high-resolution lake record from the central Northwest Territories. *PLoS One*, 13(6), e0199872. <https://doi.org/10.1371/journal.pone.0199872>
- Dean, R. G., & Dalrymple, R. A. (1991). Water wave mechanics for engineers and scientists. In *Advanced Series on Ocean Engineering* (Vol. 2). World Scientific. ISBN 978-981-02-0420-4.
- Denomme, K., Bentley, S., & Droessler, A. (2014). Climatic controls on hurricane patterns: A 1200-y near-annual record from Lighthouse Reef, Belize. *Scientific Reports*, 4, 3876. <https://doi.org/10.1038/srep03876>
- Dietze, E., & Dietze, M. (2019). Grain-size distribution unmixing using the R package EMMAgeo. *E&G Quaternary Science Journal*, 68, 29–46. <https://doi.org/10.5194/egqsj-68-29-2019>
- Dietze, E., Hartmann, K., Diekmann, B., Ijmer, J., Lehmkühl, F., Opitz, S., et al. (2012). An end-member algorithm for deciphering modern detrital processes from lake sediments of Lake Donggi Cona, NE Tibetan Plateau, China. *Sedimentary Geology*, 243, 169–180. <https://doi.org/10.1016/j.sedgeo.2011.09.014>
- Dietze, E., Maussion, F., Ahlborn, M., Diekmann, B., Hartmann, K., Henkel, K., et al. (2014). Sediment transport processes across the Tibetan Plateau inferred from robust grain-size end-members in lake sediments. *Climate of the Past*, 10(1), 91–106. <https://doi.org/10.5194/cp-10-91-2014>
- Donnelly, J. P., Hawkes, A. D., Lane, P., MacDonald, D., Shuman, B. N., Toomey, M. R., et al. (2015). Climate forcing of unprecedented intense hurricane activity in the last 2000 years. *Earth's Future*, 3, 49–65. <https://doi.org/10.1002/2014ef000274>
- Donnelly, J. P., Roll, S., Wengren, M., Butler, J., Lederer, R., & Webb, T., III. (2001). Sedimentary evidence of intense hurricane strikes from New Jersey. *Geology*, 29(7), 615–618. [https://doi.org/10.1130/0091-7613\(2001\)029<0615:seoih>2.0.co;2](https://doi.org/10.1130/0091-7613(2001)029<0615:seoih>2.0.co;2)
- Dostal, J., van Hengstum, T. R., Shellnutt, J. G., & Hanley, J. J. (2016). Petrogenetic evolution of Late Paleozoic rhyolites of the Harvey Group, southwestern New Brunswick (Canada) hosting uranium mineralization. *Contributions to Mineralogy and Petrology*, 171, 59. <https://doi.org/10.1007/s00410-016-1270-8>
- Dypvik, H., & Harris, N. B. (2001). Geochemical facies analysis of fine grained siliciclastics using Th/U, Zr/Rb and (Zr/Rb)/Sr ratios. *Chemical Geology*, 181, 131–146. [https://doi.org/10.1016/S0009-2541\(01\)00278-9](https://doi.org/10.1016/S0009-2541(01)00278-9)
- El-Jabi, N., Turkan, N., & Caissis, D. (2013). Regional climate Index for floods and droughts using Canadian Climate Model (CGCM3.1). *American Journal of Climate Change*, 2, 106–115. <https://doi.org/10.4236/ajcc.2013.22011>
- Emery, K. O. (1969). A coastal pond studied by oceanographic methods. Oyster Pond Environmental Trust Inc., (p. 111).
- Evans, G., Augustinus, P., Gadd, P., Zawadzki, A., Ditchfield, A., & Hopkins, J. (2021). A multi-proxy paleoenvironmental interpretation spanning the last glacial cycle (ca. 117 ± 8.5 ka BP) from a lake sediment stratigraphy from Lake Kai Iwi, Northland, New Zealand. *Journal of Paleolimnology*, 65, 101–122. <https://doi.org/10.1007/s10933-020-00151-z>
- Fagan, B. (2001). The Little Ice Age: How climate made history (1300–1850). Basic Books (p. 272). ISBN-10: 0465022723.
- Gallagher, E., Wadman, H., McNinch, J., Reniers, A., & Koktas, M. (2016). A conceptual model for spatial grain size variability on the surface of and within beaches. *Journal of Marine Science and Engineering*, 4(2), 38. <https://doi.org/10.3390/jmse4020038>
- Gammon, P. R., Neville, L. A., Patterson, R. T., Savard, M. M., & Swindles, G. T. (2017). A log-normal spectral analysis of inorganic grain-size distributions from a Canadian boreal lake core: Towards refining depositional process proxy data from high latitude lakes. *Sedimentology*, 64, 609–630. <https://doi.org/10.1111/sed.12281>
- Glew, J. R., Smol, J. P., & Last, W. M. (2001). Sediment core collection and extrusion. In W. M. Last, & J. P. Smol (Eds.), *Tracking environmental change using lake sediments. Vol 1: Basin analysis, coring, and chronological techniques* (pp. 73–105). Kluwer Academic Publishers.
- Government of New Brunswick Flood History Database. (2012). Created in 2012 and periodically updated. Retrieved from <http://www.elgegl.gnb.ca/0001/en/Flood/Search>
- Gray, L. J., Anstey, J. A., Kawatani, Y., Lu, H., Osprey, S., & Schenzinger, V. (2018). Surface impacts of the quasi biennial oscillation. *Atmospheric Chemistry and Physics*, 18(11), 8227–8247. <https://doi.org/10.5194/acp-18-8227-2018>
- Gray, L. J., Beer, J., Geller, M., Haigh, J. D., Lockwood, M., Matthes, K., et al. (2010). Solar influences on climate. *Reviews of Geophysics*, 48(4), RG4001. <https://doi.org/10.1029/2009RG000282>
- Gregory, B. R. B., Patterson, R. T., Galloway, J. M., & Reinhardt, E. G. (2021). The impact of cyclical, multi-decadal to centennial climate variability on arsenic sequestration in lacustrine sediments. *Palaeogeography, Palaeoclimatology, Palaeoecology*, 565, 110189. <https://doi.org/10.1016/j.palaeo.2020.110189>
- Gregory, B. R. B., Patterson, R. T., Reinhardt, E. G., Galloway, J. M., & Roe, H. M. (2019). An evaluation of methodologies for calibrating ITRAX X-ray fluorescence counts with ICP-MS concentration data for discrete sediment samples. *Chemical Geology*, 521, 12–27. <https://doi.org/10.1016/j.chemgeo.2019.05.008>
- Gregory, B. R. B., Reinhardt, E. G., Macumber, A. L., Nasser, N. A., Patterson, R. T., Kovacs, S. E., & Galloway, J. M. (2017). Sequential sample reservoirs for ITRAX-XRF analysis of discrete samples. *Journal of Paleolimnology*, 57, 287–293. <https://doi.org/10.1007/s10933-017-9944-4>
- Grimm, E. C. (1987). CONISS: A Fortran 77 program for stratigraphically constrained cluster analysis by the method of the incremental sum of Squares. *Computer and Geosciences*, 13, 13–35. [https://doi.org/10.1016/0098-3004\(87\)90022-7](https://doi.org/10.1016/0098-3004(87)90022-7)
- Gushulak, C. A. C., Reinhardt, E. G., & Cumming, B. F. (2021). Climate driven declines in terrestrial input over the middle and late Holocene of perched boreal lakes in northeast Ontario (Canada) and teleconnections to the North Atlantic. *Quaternary Science Reviews*, 265, 107056. <https://doi.org/10.1016/j.quascirev.2021.107056>
- Hakanson, L., & Jansson, M. (1983). *Principles of lake sedimentology* (p. 316). Springer-Verlag.

- Hathaway, D. H. (2015). The solar cycle. *Living Reviews in Solar Physics*, 12(1), 4. <https://doi.org/10.1007/lrsp-2015-4>
- Hu, Q., & Feng, S. (2012). AMO- and ENSO-driven summertime circulation and precipitation variations in North America. *Journal of Climate*, 25(19), 6477–6495. <https://doi.org/10.1175/jcli-d-11-00520.1>
- Jones, E. T., Hewlett, R., & Mackay, A. W. (2021). Weird weather in Bristol during the Grindelwald Fluctuation (1560-1630). *Weather*, 76, 104–110. <https://doi.org/10.1002/wea.3846>
- Juggins, S. (2022). *Rioja: Analysis of quaternary science data. R package version 1.0-5*. <https://cran.r-project.org/package=rioja>
- Keigwin, L. D. (1996). The Little Ice Age and Medieval warm period in the Sargasso Sea. *Science*, 274(5292), 1503–1508. <https://doi.org/10.1126/science.274.5292.1503>
- Kiani-Harchegani, M., Sadeghi, S. M., & Asadi, H. (2018). Comparing grain size distribution of sediment and original soil under raindrop detachment and raindrop-induced and flow transport mechanism. *Hydrological Sciences Journal*, 63(2), 312–323. <https://doi.org/10.1080/02626667.2017.1414218>
- Klamt, A. M., Poulsen, S. P., Odgaard, B. V., Hübener, T., McGowan, S., Jensen, H. S., & Reitzel, K. (2021). Holocene lake phosphorus species and primary producers reflect catchment processes in a small, temperate lake. *Ecological Monographs*, 91(3), e01455. <https://doi.org/10.1002/ecm.1455>
- Knapp, K. R., Kruk, M. C., Levinson, D. H., Diamond, H. J., & Neumann, C. J. (2010). The international best track archive for climate stewardship (IBTrACS). *Bulletin of the American Meteorological Society*, 364, 363–376. <https://doi.org/10.1175/2009bams2755.1>
- Knutson, T. R., McBride, J. L., Chan, J., Emanuel, K. A., Holland, G., Landsea, C., et al. (2010). Tropical cyclones and climate change. *Nature Geoscience*, 3(3), 157–163. <https://doi.org/10.1038/ngeo779>
- Kopp, G. (2014). An assessment of the solar irradiance record for climate studies. *Journal of Space Weather and Space Climate*, 4, A14. <https://doi.org/10.1051/swsc/2014012>
- Kuha, J., Arvola, L., Hanson, P. C., Huotari, J., Huttula, T., Juntunen, J., et al. (2016). Response of boreal lakes to episodic weather-induced events. *Inland Waters*, 6, 523–534. <https://doi.org/10.1080/iw-6.4.886>
- Lamb, H. H. (1995). The Little Ice Age. In *Climate, history and the modern world* (pp. 211–241). Routledge.
- Li, L., & Chakraborty, P. (2020). Slower decay of landfalling hurricanes in a warming world. *Nature*, 587, 230–234. <https://doi.org/10.1038/s41586-020-2867-7>
- Li, Z., Manson, A. H., Li, Y., & Meek, C. (2017). Circulation characteristics of persistent cold spells in central–eastern North America. *Journal of Meteorological Research*, 31(1), 250–260. <https://doi.org/10.1007/s13351-017-6146-y>
- Liu, K. (2004). Paleotemperature. In R. J. Murnane, & K.-B. Liu (Eds.), *Hurricanes and typhoons: Past, present, and future* (pp. 13–57). Columbia University Press.
- Liu, K. B., & Fearn, M. L. (1993). Lake-sediment record of late Holocene hurricane activities from coastal Alabama. *Geology*, 21(9), 793–796. [https://doi.org/10.1130/0091-7613\(1993\)021<0793:lsrohl>2.3.co;2](https://doi.org/10.1130/0091-7613(1993)021<0793:lsrohl>2.3.co;2)
- Lo, F.-L., Chen, H.-F., & Fang, J.-N. (2017). Discussion of suitable chemical weathering proxies in sediments by comparing the dissolution rates of minerals in different rocks. *The Journal of Geology*, 125(1), 83–99. <https://doi.org/10.1086/689184>
- Lockett, J. (2012). The discovery of weather: Stephen Saxby, the tumultuous birth of weather forecasting, and Saxby's Gale of 1869. *Formac*, 272, 978–1459500808.
- Lund, D. C., Lynch-Stieglitz, J., & Curry, W. B. (2006). Gulf Stream density structure and transport during the past millennium. *Nature*, 444(7119), 601–604. <https://doi.org/10.1038/nature05277>
- Lyu, K., & Yu, J.-Y. (2017). Climate impacts of the Atlantic Multidecadal Oscillation simulated in the CMIP5 models: A re-evaluation based on a revised index. *Geophysical Research Letters*, 44(8), 3867–3876. <https://doi.org/10.1002/2017gl072681>
- Macumber, A. L., Patterson, R. T., Galloway, J. M., Falck, H., & Swindles, G. T. (2018). Reconstruction of Holocene hydroclimatic variability in subarctic treeline lakes using lake sediment grain-size end-members. *The Holocene*, 28, 845–857. <https://doi.org/10.1177/0959683617752836>
- Mallinson, D. J., Smith, C. W., Mahan, S., Culver, S. J., & McDowell, K. (2011). Barrier island response to late Holocene climate events, North Carolina, USA. *Quaternary Research*, 76(1), 46–57. <https://doi.org/10.1016/j.yqres.2011.05.001>
- Mann, M. E., Woodruff, J. D., Donnelly, J. P., & Zhang, Z. (2009). Atlantic hurricanes and climate over the past 1,500 years. *Nature*, 460, 880–883. <https://doi.org/10.1038/nature08219>
- Mantua, N. J., & Hare, S. R. (2002). The Pacific decadal oscillation. *Journal of Oceanography*, 58(1), 35–44. <https://doi.org/10.1023/a:1015820616384>
- Marcott, S. A., Shakun, J. D., Clark, P. U., & Mix, A. C. (2013). A reconstruction of regional and global temperature for the past 11,300 years. *Science*, 339, 1198–1201. <https://doi.org/10.1126/science.1228026>
- Maslin, M., Stickley, C., & Ettwein, V. (2019). Holocene climate variability. *Encyclopedia of Ocean Sciences (Third Edition)*, 4, 513–519. <https://doi.org/10.1016/b978-0-12-409548-9.10788-2>
- Matthews, J. A., & Briffa, K. R. (2005). 'The Little Ice Age': Re-evaluation of an evolving concept. *Geografiska Annaler Series A Physical Geography*, 87A, 7–36. <https://doi.org/10.1111/j.0435-3676.2005.00242.x>
- McKerrow, W. S., & Ziegler, A. M. (1971). The Lower Silurian paleogeography of New Brunswick and adjacent areas. *The Journal of Geology*, 79(6), 635–646. <https://doi.org/10.1086/627695>
- McNeill-Jewer, C. A., Reinhardt, E. G., Collins, S., Kovacs, S., Chan, W. M., Devos, F., & LeMaillot, C. (2019). The effect of seasonal rainfall on nutrient input and biological productivity in the Yax Chen cave system (Ox Bel Ha), Mexico, and implications for μ XRF core studies of paleohydrology. *Palaeoecology, Palaeoclimatology, Palaeoecology*, 534, 109289. <https://doi.org/10.1016/j.palaeo.2019.109289>
- McWilliams, D. (1963). *Early American Hurricanes 1492-1870* (p. 212). American Meteorological Society.
- Moreno-Chamarro, E., Ortega, P., González-Rouco, J. F., & Montoya, M. (2017). Assessing reconstruction techniques of the Atlantic Ocean circulation variability during the last millennium. *Climate Dynamics*, 48(3–4), 1–21. <https://doi.org/10.1007/s00382-016-3111-x>
- Moreno-Chamarro, E., Zanchettin, D., Lohmann, K., & Jungclauss, J. H. (2015). Internally generated decadal cold events in the northern North Atlantic and their possible implications for the demise of the Norse settlements in Greenland. *Geophysical Research Letters*, 42(3), 908–915. <https://doi.org/10.1002/2014gl062741>
- Moreno-Chamarro, E., Zanchettin, D., Lohmann, K., & Jungclauss, J. H. (2017). An abrupt weakening of the subpolar gyre as trigger of Little Ice Age-type episodes. *Climate Dynamics*, 48, 724–744. <https://doi.org/10.1007/s00382-016-3106-7>
- Moreno-Chamarro, E., Zanchettin, D., Lohmann, K., Luterbacher, J., & Jungclauss, J. H. (2017). Winter amplification of the European Little Ice Age cooling by the subpolar gyre. *Scientific Reports*, 7, 339–438. <https://doi.org/10.1038/s41598-017-07969-0>
- Mullaugh, K. M., Wiley, J. D., Kieber, R. J., Mead, R. N., & Avery, G. B., Jr. (2013). Dynamics of the chemical composition of rainwater throughout Hurricane Irene. *Atmosphere Chemistry and Physics*, 13, 2321–2330. <https://doi.org/10.5194/acp-13-2321-2013>
- Murray, M. R. (2002). Is laser particle size determination possible for carbonate-rich lake sediments? *Journal of Paleolimnology*, 27, 173–183. <https://doi.org/10.1023/a:1014281412035>

- Neukom, R., Steiger, N., Gómez-Navarro, J. J., Wang, J., & Werner, J. P. (2019). No evidence for globally coherent warm and cold periods over the preindustrial common era. *Nature*, *571*(7766), 550–554. <https://doi.org/10.1038/s41586-019-1401-2>
- NOAA. (2021). NOAA historical hurricane tracks. Retrieved from <https://oceanservice.noaa.gov/news/historical-hurricanes/>
- Oliva, F., Peros, M., & Viau, A. (2017). A review of the spatial distribution of and analytical techniques used in paleotempestological studies in the western North Atlantic Basin. *Progress in Physical Geography*, *41*, 171–190. <https://doi.org/10.1177/0309133316683899>
- Oliva, F., Peros, M., Viau, A. E., Reinhardt, E. G., Nixon, F. C., & Morin, A. (2018). A multi-proxy reconstruction of tropical cyclone variability during the past 800 years from Robinson Lake, Nova Scotia, Canada. *Marine Geology*, *406*, 84–97. <https://doi.org/10.1016/j.margeo.2018.09.012>
- Oliva, F., Viau, A. E., Person, M. C., & Bouchard, M. (2018). Paleotempestology database for the Western North Atlantic basin. *The Holocene*, *28*(10), 1664–1671. <https://doi.org/10.1177/0959683618782598>
- Olsen, J., Anderson, N. J., & Knudsen, M. F. (2012). Variability of the North Atlantic Oscillation over the past 5,200 years. *Nature Geoscience*, *5*(11), 808–812. <https://doi.org/10.1038/ngeo1589>
- Pajari, G. E. (1973). The Harvey volcanic area. In N. Rast (Ed.), *Geology of New Brunswick, Field Guide to Excursions* (pp. 119–123). New England Intercollegiate Geological Conference, Department of Geology, University of New Brunswick, Trip A-14 and B-11.
- Parker, G. (2018). History and climate: The crisis of the 1590s reconsidered. In C. Leggewie, & F. Mauelshagen (Eds.), *Climate change and cultural transition in Europe* (pp. 119–155). Brill.
- Parris, A. S., Bierman, P. R., Noren, A. J., Prins, M. A., & Lini, A. (2010). Holocene paleostorms identified by particle size signatures in lake sediments from the northeastern United States. *Journal of Paleolimnology*, *43*, 29–49. <https://doi.org/10.1007/s10933-009-9311-1>
- Patterson, R. T. (2022). A 520-year paleolimnological grain size and ITRAX record from Harvey Lake, New Brunswick, Canada [Dataset]. Dryad. <https://doi.org/10.5061/dryad.8cz8w9gpw>
- Patterson, R. T., Mazzella, V., Macumber, A. L., Gregory, B. R. B., Patterson, C. W., Nasser, N. A., et al. (2020). A novel protocol for mapping the spatial distribution of storm derived sediment in lakes. *SN Applied Sciences*, *2*, 2125. <https://doi.org/10.1007/s42452-020-03908-3>
- Patterson, R. T., & Swindles, G. T. (2015). Influence of ocean–atmospheric oscillations on lake ice phenology in eastern North America. *Climate Dynamics*, *45*(9–10), 2293–2308. <https://doi.org/10.1007/s00382-014-2415-y>
- Peng, Y., Xiao, J., Nakamura, T., Liu, B., & Inouchi, Y. (2005). Holocene East Asian monsoonal precipitation pattern revealed by grain-size distribution of core sediments of Daihai Lake in Inner Mongolia of north-central China. *Earth and Planetary Science Letters*, *233*, 467–479. <https://doi.org/10.1016/j.epsl.2005.02.022>
- Peros, M., Collins, S., G’Meiner, A. A., Reinhardt, E. G., & Pupo, F. M. (2017). Multistage 8.2 kyr event revealed through high-resolution XRF core scanning of Cuban sinkhole sediments. *Geophysical Research Letters*, *44*. <https://doi.org/10.1002/2017gl074369>
- R Core Team. (2020). *R: A language and environment for statistical computing*. R Foundation for Statistical Computing. Retrieved from <https://www.R-project.org/>
- Reimer, P., Austin, W., Bard, E., Bayliss, A., Blackwell, P. G., Ramsey, C. B., et al. (2020). The IntCal20 Northern Hemisphere radiocarbon age calibration curve (0–55 cal kBP). *Radiocarbon*, *62*(4), 725–757. <https://doi.org/10.1017/rdc.2020.41>
- Roberts, N., Allcock, S. L., Arnaud, F., Dean, J. R., Eastwood, W. J., Jones, M. D., et al. (2016). A tale of two lakes: A multi-proxy comparison of Lateglacial and Holocene environmental change in Cappadocia, Turkey. *Journal of Quaternary Science*, *31*(4), 348–362. <https://doi.org/10.1002/jqs.2852>
- Ruiz-Barradas, A., Nigam, S., & Kavvada, A. (2013). The Atlantic Multidecadal Oscillation in twentieth century climate simulations: Uneven progress from CMIP3 to CMIP5. *Climate Dynamics*, *41*(11–12), 3301–3315. <https://doi.org/10.1007/s00382-013-1810-0>
- Saenger, C., Cohen, A. L., Oppo, D. W., Halley, R. B., & Carilli, J. E. (2009). Surface-temperature trends and variability in the low-latitude North Atlantic since 1552. *Nature Geoscience*, *2*, 492–495. <https://doi.org/10.1038/NCEO552>
- Sakihama, H., & Tokuyama, A. (2005). Effect of typhoon on chemical composition of rainwater, Okinawa Island, Japan. *Atmospheric Environment*, *39*, 2879–2888. <https://doi.org/10.1016/j.atmosenv.2004.12.043>
- Schurer, A. P., Tett, S. F. B., & Hegerl, G. C. (2013). Small influence of solar variability on climate over the past millennium. *Nature Geoscience*, *7*, 104–108. <https://doi.org/10.1038/ngeo2040>
- Sheets, R. C. (1990). The National Hurricane Center – Past, present, and future. *Weather and Forecasting*, *5*, 185–232. [https://doi.org/10.1175/1520-0434\(1990\)005<0185:tnhcca>2.0.co;2](https://doi.org/10.1175/1520-0434(1990)005<0185:tnhcca>2.0.co;2)
- Skwira, G. D., Schroeder, J. L., & Peterson, R. E. (2005). Surface observations of landfalling hurricane records. *Monthly Weather Review*, *133*, 454–465. <https://doi.org/10.1175/mwr-2866.1>
- Sobek, S., Durisch-Kaiser, E., Zurbrugg, R., Wongfun, N., Wessels, M., Pasche, N., & Wehrli, B. (2009). Organic carbon burial efficiency in lake sediments controlled by oxygen exposure time and sediment source. *Limnology & Oceanography*, *54*, 2243–2254. <https://doi.org/10.4319/lo.2009.54.6.2243>
- Spence, C., & Woo, M. (2008). Hydrology and the northwestern Canadian Shield. In M. Woo (Ed.), *Cold region atmospheric and hydrologic studies: The Mackenzie GEWEX experience – Volume 2: Hydrologic processes* (pp. 235–256). Springer. https://doi.org/10.1007/978-3-540-75136-6_13
- Stockwell, J. D., Doubek, J. P., Adrian, R., Anneville, O., Carey, C. C., Carvalho, L., et al. (2020). Storm impacts on phytoplankton community dynamics in lakes. *Global Change Biology*, *26*, 2756–2784. <https://doi.org/10.1111/gcb.15033>
- Studholme, J., Federov, A. V., Gulev, S. K., Emanuel, K., & Hodges, K. (2022). Poleward expansion of tropical cyclone latitudes in warming climates. *Nature Geoscience*, *15*, 14–28. <https://doi.org/10.1038/s41561-021-00859-1>
- Swindles, G. T., Galloway, J. M., Macumber, A. L., Croudace, I. W., Emery, A. R., Woudes, C., et al. (2018). Sedimentary records of coastal storm surges: Evidence of the 1953 North Sea event. *Marine Geology*, *403*, 262–270. <https://doi.org/10.1016/j.margeo.2018.06.013>
- Taylor, R. E. (1987). *Radiocarbon dating: An archaeological perspective* (p. 212). Academic Press.
- Thibodeau, B., Not, C., Zhu, J., Schmittner, A., Noone, D., Tabor, C., et al. (2018). Last century warming over the Canadian Atlantic shelves linked to weak Atlantic meridional overturning circulation. *Geophysical Research Letters*, *45*, 12376–12385. <https://doi.org/10.1029/2018gl080083>
- Thirumalai, K., Quinn, T. M., Okumura, Y., Richey, J. N., Partin, J. W., Poore, R. Z., & Moreno-Chamarro, E. (2018). Pronounced centennial-scale Atlantic Ocean climate variability correlated with Western Hemisphere hydroclimate. *Nature Communications*, *9*, 392. <https://doi.org/10.1038/s41467-018-02846-4>
- van de Plassche, O., Erkens, G., van Vliet, F., Brandsma, J., van der Borg, K., & de Jong, A. F. (2006). Salt-marsh erosion associated with hurricane landfall in southern New England in the fifteenth and seventeenth centuries. *Geology*, *34*(10), 829–832. <https://doi.org/10.1130/g22598.1>
- van Hengstum, P. J., Donnelly, J. P., Toomey, M. R., Albury, N. A., Lane, P., & Kakuk, B. (2013). Heightened hurricane activity on the Little Bahama Bank from 1350 to 1650 AD. *Continental Shelf Research*, *86*, 103–115.
- van Hengstum, P. J., Reinhardt, E. G., Boyce, J. I., & Clark, C. (2007). Changing sedimentation patterns due to historical land-use change in Frenchman’s Bay, Pickering, Canada: Evidence from high-resolution textural analysis. *Journal of Paleolimnology*, *37*, 603–618. <https://doi.org/10.1007/s10933-006-9057-y>

- Wallace, D. J., Woodruff, J. D., Anderson, J. B., & Donnelly, J. P. (2014). Palaeohurricane reconstructions from sedimentary archives along the Gulf of Mexico, Caribbean Sea and Western North Atlantic Ocean margins. *Geological Society, London, Special Publications*, 388(1), 481–501. <https://doi.org/10.1144/sp388.12>
- Wallace, E. J., Coats, S., Emanuel, K. A., & Donnelly, J. P. (2020). Centennial-scale shifts in storm frequency captured in paleohurricane records from The Bahamas arise predominantly from random variability. *Geophysical Research Letters*, 47, e2020GL091145. <https://doi.org/10.1029/2020GL091145>
- Walsh, C. R., & Patterson, R. T. (2022b). Attribution of observed periodicity in extreme weather events in eastern North America. *Earth and Space Science*, 9, e2022EA002359. <https://doi.org/10.1029/2022EA002359>
- Walsh, C. R., & Patterson, R. T. (2022a). Regional impact of large-scale climate oscillations on ice out variability in New Brunswick and Maine. *PeerJ*, 10, e13741. <https://doi.org/10.7717/peerj.13741>
- Wanamaker, A. D., Kreutz, K. J., Schöne, B. R., Pettigrew, N., Borns, H. W., Introne, D. S., et al. (2008). Coupled North Atlantic slope water forcing on Gulf of Maine temperatures over the past millennium. *Climate Dynamics*, 31, 183–194. <https://doi.org/10.1007/s00382-007-0344-8>
- Weltje, G. J., Bloemsa, M. R., Tjallingii, R., Heslop, D., Röhl, U., & Croudace, I. W. (2015). Prediction of geochemical composition from XRF core scanner data: A new multivariate approach including automatic selection of calibration samples and quantification of uncertainties. In I. W. Croudace, & R. G. Rothwell (Eds.), *Micro-XRF studies of sediment cores* (pp. 507–534). Springer Netherlands. https://doi.org/10.1007/978-94-017-9849-5_21
- Weltje, G. J., & Prins, M. A. (2003). Muddled or mixed? Inferring palaeoclimate from size distributions of deep-sea clastics. *Sedimentary Geology*, 162, 39–62. [https://doi.org/10.1016/S0037-0738\(03\)00235-5](https://doi.org/10.1016/S0037-0738(03)00235-5)
- Weltje, G. J., & Prins, M. A. (2007). Genetically meaningful decomposition of grain-size distributions. *Sedimentary Geology*, 202, 409–424. <https://doi.org/10.1016/j.sedgeo.2007.03.007>
- Whitney, N. M., Wanamaker, A. D., Ummenhofer, C. C., Johnson, B. J., & Cresswell-Clay, N. (2022). Rapid 20th century warming reverses 900-year cooling in the Gulf of Maine. *Communications Earth & Environment*, 3, 179. <https://doi.org/10.1038/s43247-022-00504-8>
- Wilson, S. G., & Fischetti, T. R. (2010). Coastal population trends in the United States: 1960–2008. US Census Bureau Current Population Reports P25-1139, (p. 28).
- Winkler, T. S., van Hengstum, P. J., Donnelly, J. P., Wallace, E. J., Sullivan, R. M., MacDonald, D., & Albury, N. A. (2020). Revising evidence of hurricane strikes on Abaco Island (The Bahamas) over the last 700 years. *Scientific Reports*, 10(1), 1–17. <https://doi.org/10.1038/s41598-020-73132-x>
- Yang, Y., Maselli, V., Normandeau, A., Piper, D. J. W., Li, M. Z., Campbell, D. C., et al. (2020). Latitudinal response of storm activity to abrupt climate change during the last 6,500 years. *Geophysical Research Letters*, 47, e2020GL089859. <https://doi.org/10.1029/2020GL089859>
- Zeng, A., Zhou, X., Li, Z., Chen, F., Luo, H., He, G., et al. (2022). Influence of typhoons on chemical makeup of rainwater in Zhanjiang, China. *Aerosol and Air Quality Research*, 22(3), 210210. <https://doi.org/10.4209/aaqr.210210>
- Zhang, R., & Vallis, G. K. (2007). The role of bottom vortex stretching on the path of the North Atlantic Western Boundary Current and on the Northern Recirculation Gyre. *Journal of Physical Oceanography*, 37, 2053–2080. <https://doi.org/10.1175/jpo3102.1>